

Highlights

A new branch-and-cut approach for integrated planning in additive manufacturing

Benedikt Zipfel, Felix Tamke, Leopold Kuttner

- We present a new exact algorithm for a scheduling problem in additive manufacturing.
- We extend state-of-the-art techniques to solve the orthogonal packing with rotation.
- The branch-and-cut algorithm is vastly superior to an existing integrated model.
- We propose new benchmark instances for the considered planning problem.

A new branch-and-cut approach for integrated planning in additive manufacturing

Benedikt Zipfel^{a,*}, Felix Tamke^a and Leopold Kuttner^a

^aDepartment of Business Administration, esp. Industrial Management, Helmholtzstraße 10, Dresden, 01069, Saxony, Germany

ARTICLE INFO

ABSTRACT

Keywords:

Scheduling

Unrelated machines

Orthogonal packing

Additive manufacturing

Branch-and-cut


In recent years, there has been considerable interest in the transformative potential of additive manufacturing (AM) since it allows for producing highly customizable and complex components while reducing lead times and costs. The rise of AM for traditional and new business models enforces the need for efficient planning procedures for AM facilities. In this area, the assignment and sequencing of components to be built by an AM machine, also called a 3D printer, is a complex problem joining the nesting and scheduling of parts to be printed. This paper proposes a new branch-and-cut algorithm for integrated planning for unrelated parallel machines. The algorithm is based on combinatorial Benders decomposition: The scheduling problem is considered in the master problem, while the feasibility of a solution is checked in the sub-problem. Current state-of-the-art techniques are extended to solve the orthogonal packing with rotation to speed up the solution of the sub-problem. Extensive computational tests on existing instances and a new benchmark instance set show the algorithm's superior performance compared to an existing integrated mixed-integer programming model.

1. Introduction

Initially, additive manufacturing (AM) was adopted to speed up time-to-market or to quickly find solutions from rapid prototyping in the pre-production phase, but it is also increasingly being used for serial production in various industries (Kang, Noh, Son, Kim, Park and Lee, 2018). The general technology, also known as 3D printing, can be described as the process of building up parts layer by layer, based on a digital data model (Thompson, Moroni, Vaneker, Fadel, Campbell, Gibson, Bernard, Schulz, Graf, Ahuja and Martina, 2016). AM technologies do not require prior tooling activities (Attaran, 2017) and are able to process several parts simultaneously in the same production step (Kucukkoc, 2019). Because AM enables the building of highly complex parts, it is especially suited to customization purposes (Guo and Leu, 2013). While research initially studied the technologies and processes, recent studies increasingly focus on production planning aspects of AM (Oh, Witherell, Lu and Sprock, 2020). The growing interest in production planning is partly driven by new on-demand services, such as Factory-as-a-Service and Production-as-a-Service, that are based on AM technologies (see, e.g., Kang et al. (2018)). However, efficient planning and operations management are also essential for traditional industries shifting from prototypical usage of AM technologies to application in series production.

This study addresses the integrated planning problem on AM machines, which incorporates the nesting of parts into batches and the scheduling of those batches on the available machines (Manco, Macchiaroli, Maresca and Fera, 2019). As the nesting and the scheduling problem directly influence each other (Oh et al., 2020), both sub-problems should be tackled simultaneously in order to obtain adequate and high-quality planning results (Kapadia, Starly, Thomas, Uzsoy and Warsing, 2019). The necessity of an integrated solution procedure becomes even more apparent in considerations of

*Corresponding author

 benedikt.zipfel@tu-dresden.de (B. Zipfel); felix.tamke@tu-dresden.de (F. Tamke); leopold.kuttner@tu-dresden.de (L. Kuttner)

ORCID(s): 0000-0003-3750-2541 (B. Zipfel); 0000-0003-1650-8936 (F. Tamke); 0000-0002-9359-8835 (L. Kuttner)

unrelated parallel machines with different build spaces and processing times. Therefore, we propose a new integrated exact solution approach to minimize makespan in an AM environment with unrelated parallel machines. The main contributions of this paper are the following:

- We present a new branch-and-cut (B&C) solution procedure to minimize the makespan on unrelated parallel AM machines, which is based on combinatorial Benders decomposition.
- We adopt and extend several state-of-the-art techniques from the literature – such as lower bounding, relaxation, placement point strategies, and constraint programming models – to solve the sub-problem of the decomposition approach.
- We compare our approach with a similar approach from the literature and demonstrate the advantage of our algorithm in terms of computational effort and solution quality by providing more optimally solved instances in fewer computation time.
- We propose new benchmark instances for the considered planning problem and demonstrate the superior performance of the proposed approach.

Of the various AM technologies, this study focuses on powder bed fusion (PBF) techniques, due to their frequent usage in commercial applications (Gibson, Rosen, Stucker and Khorasani, 2021; Li, Kucukkoc and Zhang, 2017). Figure 1 shows a schematic illustration of the general build process of PBF technologies. A leveling roller spreads powder on the build area; then, a laser beam melts designated areas of the powder to create a layer of the part. When the laser has completed the fusion process on the current layer, the build platform is lowered, and the leveling roller brings out a new layer of powder (Gibson et al., 2021). Consequently, the processing time depends on the maximum height and the total volume that needs to be printed.

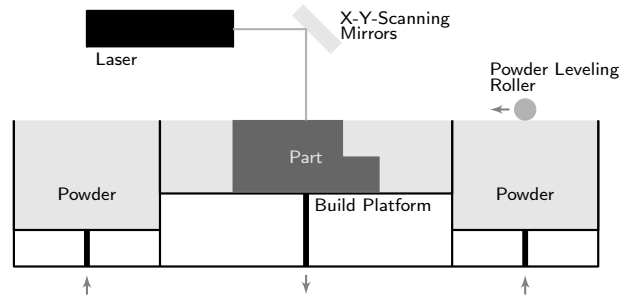


Figure 1: Generalized explanation of the print process in PBF technologies following Gardan (2017)

The nesting problem usually takes into account the placement and orientation of parts within the build area. If not all parts fit into a single build area, it is also necessary to group parts into several batches (Oh et al., 2020). In this study, we consider the bounding boxes of each part. This is illustrated in Figure 2, in which the cuboid bounding box of a model part is represented by dashed lines.

The terms 'nesting' and 'packing' are sometimes used as synonyms; however, as we understand it, nesting is associated with irregular shapes (see, e.g., Baldacci, Boschetti, Ganovelli and Maniezzo, 2014), whereas packing is mostly associated with rectangular shapes. Therefore, as this study considers cuboid bounding boxes with rectangular base areas, we use the term 'packing' in the remainder of this work. Since we do not allow the stacking of parts, each part must be connected to the build plate of a printer. Furthermore, we assume a fixed build orientation of each part, which is predefined in the design process. Parts can only be rotated 90 degrees around the z-axis. This is also illustrated in Figure 2, with both rotation variants of a model part. Consequently, the studied problem incorporates both the packing of parts as a two-dimensional bin packing problem with rotation (2D-BPR) and the scheduling of the resulting batches on the available unrelated machines. The machines differ in terms of their processing speeds and build spaces.

The remainder of this paper is organized as follows. Section 2 reviews the relevant literature in scheduling problems, packing problems, and planning for additive manufacturing. In Section 3, we define the studied problem and formulate

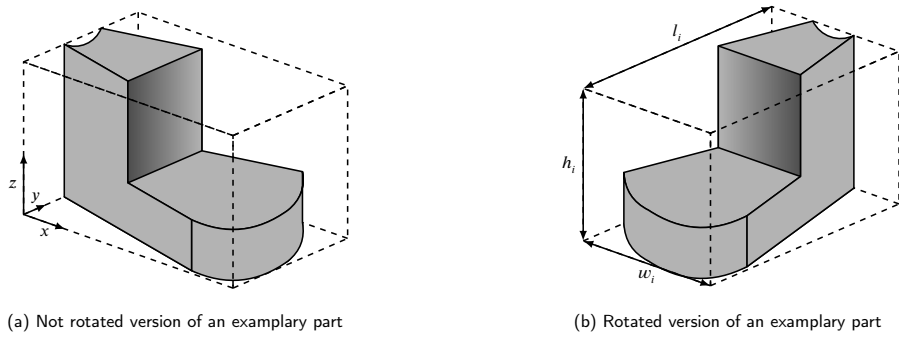


Figure 2: Illustration of the considered bounding boxes of a part

a mixed-integer linear programming model; Section 4 presents the structure of the proposed solution approach in detail. We give an overview of the general solution strategy before elaborating on the specific elements of the approach. In our computational studies in Section 5, we first analyze data from related literature, after which new benchmark test data is explained and evaluated. Finally, we conclude in Section 6 and give prospects for future research.

2. Related work

We review relevant articles from literature streams that are related to the problem configuration considered here. We first focus on batch scheduling problems; then, the review continues with relevant studies found in the packing and cutting literature. Finally, we present recent papers that explicitly consider packing and scheduling for AM.

2.1. Scheduling on batch processing machines

Scheduling on batch processing machines has been studied extensively in the recent decades. Initially, Uzsoy (1994) introduced the batch processing scheduling problem (BPSP) for a single batch processing machine; since then, several authors have extended the problem. The most relevant extensions related to the problem examined in this study are non-identical job sizes and unrelated parallel machines. Li, Huang, Tan and Chen (2013) study batch scheduling with these two extensions to minimize makespan, combining different heuristics in two-step approaches and evaluating their performance. More recently, Arroyo and Leung (2017b) propose a mathematical programming model for a similar problem, extended by unequal ready times; alongside the exact solution approach, they propose several heuristics to solve the problem. Arroyo and Leung (2017a) also address machine-dependent processing times of the parts and different machine capacities. Additionally, a combination of batch scheduling and two-dimensional bin packing is found in Polyakovskiy and M'Hallah (2021), who aim to minimize total weighted earliness and tardiness by introducing different combinations of mixed integer programming (MIP) models and constraint programming (CP) models.

Similar to the present study, Li et al. (2013) and Arroyo and Leung (2017b) take into account parts with different sizes. However, the unrelated machines in those studies differ only based on the processing times, while in our case the machines also have different capacities. In Arroyo and Leung (2017a), the authors extend their previous work and integrate varying machine sizes. All three of these articles consider a one-dimensional packing case, while the present problem assumes placement on a two-dimensional platform. A main difference between the planning problems for batch processing and AM lies in the determination of processing times: in traditional batch scheduling, the processing time of a batch is typically defined by the maximum or the sum of all job processing times, while the processing time in AM depends on the composition of a batch (Alicastro, Ferone, Festa, Fugaro and Pastore, 2021). In contrast to the work of Polyakovskiy and M'Hallah (2021), wherein the number of parts in the batch is relevant for the processing time, in AM the processing times of batches depend on the actual dimensions of the batched parts. Furthermore, our work differs from their work by considering non-guillotine packing.

2.2. Two-dimensional packing

For a comprehensive overview of two-dimensional packing literature, we refer to Iori, de Lima, Martello, Miyazawa and Monaci (2021), who provide an extensive summary of the solution approaches that investigate this problem class.

Our study falls under the category of two-dimensional bin packing problem (2D-BPP) with variable bin sizes and orthogonal rotations. Pisinger and Sigurd (2005) address 2D-BPP with variable bin sizes and propose an exact solution approach based on branch-and-price. Moreover, they present several lower bounds for the problem, including a bound based on Dantzig-Wolfe decomposition. Several publications in the packing literature discuss orthogonal rotation of parts. Here, we give special attention to those articles discussing lower bounding techniques for this problem variant. Dell'Amico, Martello and Vigo (2002) present a lower bound for 2D-BPP with rotation (2D-BPR), for which the parts are cut into squares; the new lower bounding technique is embedded in a branch-and-bound algorithm, and its efficiency against the continuous lower bound is demonstrated in a computational study. Boschetti and Mingozzi (2003) propose another lower bound by modifying part sizes. A summary of lower bounds for the 2D-BPR is presented by Clautiaux, Jouglet and El Hayek (2007b), who also present a new lower bound for the 2D-BPR if the considered bin is a square; the authors show the dominance of the newly proposed bound in computational tests. Polyakovskiy and M'Hallah (2018) present yet another bound for the 2D-BPR based on dual feasible functions (DFFs), and they show the superior performance of their bound compared to the lower bound of Clautiaux et al. (2007b) and the bound resulting from CPLEX. The study of Côté, Haouari and Iori (2021) solves the 2D-BPP with a new branch-and-cut approach based on Benders decomposition. The authors incorporate several state-of-the-art mechanisms and methods from the packing literature to improve the best-known results for the benchmark sets. While Côté et al. (2021) consider the 2D-BPP, in our work, the 2D-BPR is a sub-problem of the integrated problem configuration; furthermore, these authors do not consider the rotation of parts. Nevertheless, the ideas presented in that study significantly influenced the investigations in our paper and will therefore be referred to in different sections of this study.

2.3. Integrated planning for additive manufacturing

2.3.1. Integrated planning with one-dimensional packing

The number of studies explicitly incorporating packing and scheduling for AM is growing very quickly. Li et al. (2017) introduce a mixed-integer programming model to minimize production costs for the problem of scheduling AM machines; they add tolerances to the production areas of the parts and check whether the summed area of assigned parts is smaller than the available build area on the machine. This one-dimensional bin packing problem (1D-BPP) constraint is adopted by Kucukkoc (2019), who studies scheduling in AM for single, identical, and unrelated parallel machines: for each machine environment, the author presents an MIP model that aims to minimize makespan. Tavakkoli-Moghaddam, Shirazian and Vahedi-Nouri (2020) tackle makespan and total tardiness simultaneously in a bi-objective approach; in addition, they extend the work of Kucukkoc (2019) by considering material types, which leads to incompatibilities between products. The approach proposed by Chergui, Hadj-Hamou and Vignat (2018) considers customer orders, which are composed of several parts. In their approach, the problem is split into two sub-problems dealing with the assignment of batches and the sequencing on parallel identical machines. Zipfel, Neufeld and Buscher (2021) link the extensions of Tavakkoli-Moghaddam et al. (2020) with the order-based configuration of Chergui et al. (2018) and propose a new MIP formulation. In addition to different material types, the authors also incorporate quality levels for the ordered parts. Elsewhere, a matheuristic for minimizing total weighted tardiness is proposed by Rohaninejad, Hanzálek and Tavakkoli-Moghaddam (2021), who present a combination of a genetic algorithm and a local search based on an MIP model: the machine assignment is addressed in the genetic algorithm, while the MIP-based local search takes care of assigning parts to batches. In Alicastro et al. (2021), an iterated local search is combined with reinforcement learning; the authors further adopt heuristic approaches from strip packing problems to place the parts within the available batches.

2.3.2. Integrated planning with two-dimensional packing

What all mentioned approaches for integrated planning in AM have in common is that they use a 1D-BPP constraint instead of explicitly solving the packing problem. This can be a valid assumption if parts are large compared to the build area. However, to meet real-world requirements, the specific dimensions of the parts must be taken into account. Che, Hu, Zhang and Lim (2021) introduce an MIP model that incorporates the scheduling problem, and a two-dimensional packing problem that considers the placement and the orientation of cuboid parts with a rectangular base area on the build area. The orientation variants of each part are predefined by selected rotation movements around the x- and y-axes, while rotations around the z-axis are considered in the model formulation. The model handles orientations around the x- and y-axes using a constraint that allows only one orientation variant of each part to be placed. In addition to the mathematical model, Che et al. (2021) present a simulated annealing procedure, which they combine with different packing strategies and post-optimization methods; in a comprehensive computational test, they show the efficiency of

their developed algorithms. In Hu, Che and Zhang (2022), the aforementioned problem is extended by unequal release dates of parts; the authors adapt the MIP model presented in Che et al. (2021) and incorporate constraints to account for the extended problem configuration. Furthermore, they use an adaptive large neighborhood search to solve large-scale instances of the problem. Zhang, Yao and Li (2020) consider an integrated approach with nesting of irregularly-shaped parts. First, they present a mathematical formulation, before proposing a population-based metaheuristic that integrates the principles of no-fit polygons and inner-fit polygons.

In this study, we examine minimizing makespan on unrelated batch processing machines in AM, where the batching of parts is represented by a two-dimensional bin packing problem with rotation and variably-sized bins. This problem configuration is an extension of the planning situation seen in Kucukkoc (2019) as well as a special case of the problem in Che et al. (2021) and Hu et al. (2022). The studied scheduling sub-problem is a generalization of single batch processing machine scheduling, which has been proven to be NP-hard for minimizing makespan (Uzsoy, 1994). Furthermore, the packing sub-problem can be reduced to the 1D-BPP; therefore, it is also strongly NP-hard. While most existing work on integrated planning for AM with two-dimensional packing focuses on developing heuristic approaches, in this work, we explicitly focus on creating an exact approach. Conceptually, the procedures build on and extend the methodology in the literature of packing problems presented in Subsection 2.2. The next section gives a description of the problem configuration, followed by a mathematical formulation.

3. Problem description

3.1. Assumptions

For the studied problem, we make the following assumptions:

- All information regarding parts and machines is known and deterministic.
- We consider 3D printers with PBF technology as unrelated parallel machines that may vary in terms of their sizes and production parameters.
- All printers are available from the beginning of the planning period and there are no breakdowns of production or malfunctions.
- We consider each part using its bounding box and the respective dimensions (see Figure 2).
- Each part has a predefined build orientation and is only allowed to rotate 90 degrees around the z-axis.
- The volume of a part can be smaller than the cuboid volume of the bounding box of its width, length, and height.
- The machines are able to build several parts simultaneously in batches, and we do not allow the stacking of parts within the build spaces.
- A part needs to be assigned to exactly one batch on one specific machine.
- As soon as the production of a batch starts, no part can be added to or removed from the batch before the printing process has ended.
- The maximum number of batches is equal to the total number of parts on each machine, to guarantee feasibility.

By considering the bounding boxes of the parts, we aim to ensure consistent part quality by reducing interference of parts with each other. Furthermore, the build orientation of a part has a significant impact on the later quality of the produced component. Therefore, orientation in the build space is often determined in an earlier process step (Kucukkoc, 2019). Different materials can be used in PBF technology, and depending on the material and the associated need for additional support structures, the stacking of parts is possible (Bain, 2019). In order to attain general applicability, we assume that support structures are required, and thus stacking parts is not permitted. This assumption is important, since it distinguishes between a three-dimensional and a two-dimensional packing. However, we still need to ensure that a part also fits into the build envelope in terms of its height.

3.2. Problem definition

Let $\mathcal{I} = \{1, 2, \dots, I\}$ be a set of parts, each of which is defined by its width ω_i , length λ_i , and height η_i , $i \in \mathcal{I}$. Additionally, we are given a set $\mathcal{M} = \{1, 2, \dots, M\}$ of machines, which use PBF technology. The build envelope of an

AM machine $m \in \mathcal{M}$ is defined by its width Ω_m , length Λ_m , and height H_m . Besides their variegated build spaces, 3D printers also differ in terms of production times, which can be divided into setup time T_m^S , recoating time T_m^R , and scanning time T_m^L (Kucukkoc, 2019). The recoating time refers to the time to apply a height unit of powder onto the build area, while the scanning time refers to the time the laser needs to build one volume unit. The left side of Figure 3 illustrates a model instance of the studied problem with ten parts and two machines, and the right side of the figure presents a possible solution for this. Three batches have been created from the ten parts, based on the available build space of the machines, and those batches are sequenced on the two machines. It should be noted that we numbered the batches in ascending order for each machine – for example, Batch_{1,1} is the first batch on the first machine.

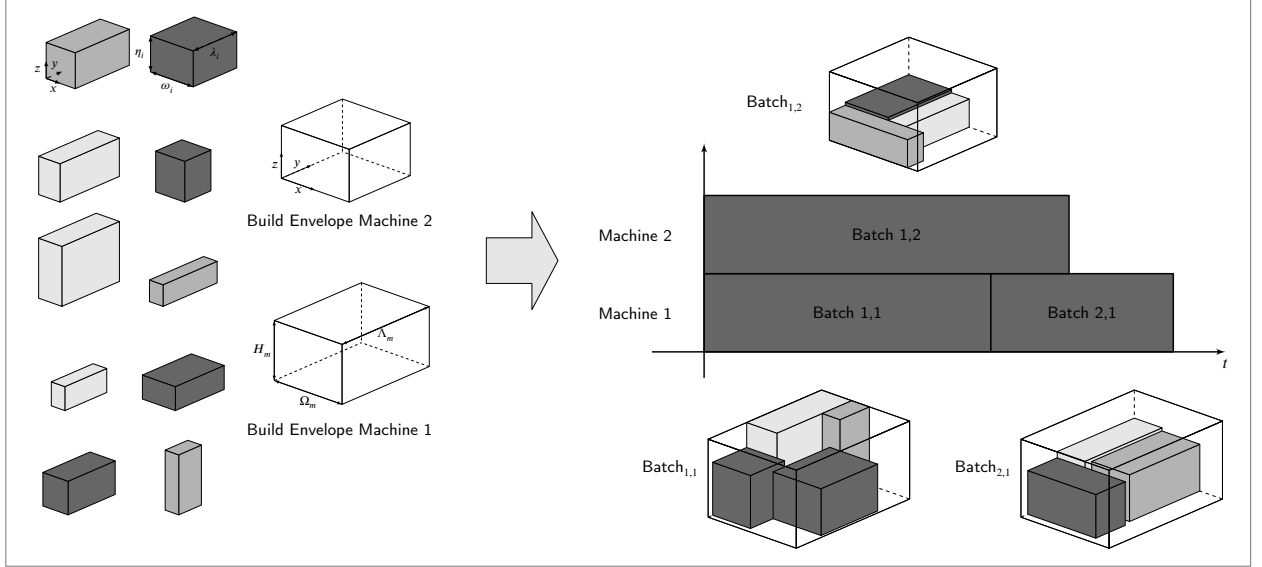


Figure 3: Example problem instance and its solution for the considered problem

In line with the example in Figure 3, the studied problem consists of assigning each part $i \in \mathcal{I}$ to exactly one machine $m \in \mathcal{M}$, packing those parts into a set of batches $\mathcal{B} = \{1, 2, \dots, B\}$, placing them within the respective build spaces, and sequencing the resulting batches on the machines. The objective is to minimize the makespan C_{\max} in a machine environment of unrelated parallel machines.

3.3. Problem formulation

To describe the studied problem mathematically, we modify the formulation of Kucukkoc (2019) by incorporating the ideas of Côté et al. (2021) for the 2D-BPP. Before modeling the problem, we give a complete description of the used notation:

Classes & Sets			
\mathcal{B}	Set of batches	\mathcal{I}	Set of parts
\mathcal{M}	Set of machines	S	Generic subset of parts, $S \subseteq \mathcal{I}$
\mathcal{T}_m	Class of infeasible subsets for part assignments to machine m	\mathcal{U}	Set of tuples (i, m) , $i \in \mathcal{I}, m \in \mathcal{M}$, if i cannot be placed on m
Parameters			
α_i	Production area of part $i \in \mathcal{I}$	H_m	Height of machine $m \in \mathcal{M}$
η_i	Height of part $i \in \mathcal{I}$	Λ_m	Length of machine $m \in \mathcal{M}$
λ_i	Length of part $i \in \mathcal{I}$	Ω_m	Width of machine $m \in \mathcal{M}$
v_i	Volume of part $i \in \mathcal{I}$	T_m^L	Scanning time for one volume unit on machine $m \in \mathcal{M}$

ω_i	Width of part $i \in \mathcal{I}$	T_m^R	Recoating time for one height unit on machine $m \in \mathcal{M}$
A_m	Area of machine $m \in \mathcal{M}$	T_m^S	Setup time on machine $m \in \mathcal{M}$
Decision Variables			
c_{bm}	Completion time of batch $b \in \mathcal{B}$ on machine $m \in \mathcal{M}$	x_{ibm}	1, if part $i \in \mathcal{I}$ is assigned to batch $b \in \mathcal{B}$ on machine $m \in \mathcal{M}$
h_{bm}	Height of batch $b \in \mathcal{B}$ on machine $m \in \mathcal{M}$	C_{\max}	Makespan
y_{bm}	1, if batch $b \in \mathcal{B}$ is processed on machine $m \in \mathcal{M}$		

With this notation on hand, the studied problem can be stated as an MIP model as follows:

$$C_{\max} \rightarrow \min \quad (1)$$

s.t.:

$$C_{\max} \geq c_{bm} \quad \forall b \in \mathcal{B}, m \in \mathcal{M}, \quad (2)$$

$$\sum_{b \in \mathcal{B}} \sum_{m \in \mathcal{M}} x_{ibm} = 1 \quad \forall i \in \mathcal{I}, \quad (3)$$

$$x_{ibm} \leq y_{bm} \quad \forall i \in \mathcal{I}, b \in \mathcal{B}, m \in \mathcal{M}, \quad (4)$$

$$h_{bm} \geq \eta_i \cdot x_{ibm} \quad \forall i \in \mathcal{I}, b \in \mathcal{B}, m \in \mathcal{M}, \quad (5)$$

$$h_{bm} \leq \max_{i \in \mathcal{I}} \{\eta_i\} \cdot y_{bm} \quad \forall b \in \mathcal{B}, m \in \mathcal{M}, \quad (6)$$

$$x_{ibm} = 0 \quad \forall b \in \mathcal{B}, i \in \mathcal{I}, m \in \mathcal{M}, (i, m) \in \mathcal{U}, \quad (7)$$

$$c_{1,m} \geq y_{1,m} \cdot T_m^S + T_m^L \cdot \sum_{i \in \mathcal{I}} (v_i \cdot x_{i,1,m}) + T_m^R \cdot h_{1,m} \quad \forall m \in \mathcal{M}, \quad (8)$$

$$c_{bm} \geq c_{b-1,m} + y_{bm} \cdot T_m^S + T_m^L \cdot \sum_{i \in \mathcal{I}} (v_i \cdot x_{ibm}) + T_m^R \cdot h_{bm} \quad \forall b \in \mathcal{B}, b > 1, m \in \mathcal{M}, \quad (9)$$

$$\sum_{i \in S} x_{ibm} \leq |S| - 1 \quad \forall b \in \mathcal{B}, m \in \mathcal{M}, S \in \mathcal{T}_m, \quad (10)$$

$$x_{ibm} \in \{0, 1\}, y_{bm} \in \{0, 1\} \quad \forall i \in \mathcal{I}, b \in \mathcal{B}, m \in \mathcal{M}, \quad (11)$$

$$C \in \mathbb{R}^+, c_{bm} \in \mathbb{R}^+ \quad \forall b \in \mathcal{B}, m \in \mathcal{M}, \quad (12)$$

$$h_{bm} \in \mathbb{N}^0 \quad \forall b \in \mathcal{B}, m \in \mathcal{M}. \quad (13)$$

The objective function defined in (1) minimizes the makespan, while constraints (2) set the makespan to be greater than or equal to all completion times of batches on the available machines. Constraints (3) ensure that each part is assigned to exactly one batch. Constraints (4) link variables x and y and establish that batch b is processed on machine m if any part i is assigned to this batch. Inequalities (5) and (6) limit the height of a batch on a machine h_{bm} to the maximum height of any part i assigned to it. A tuple $(i, m) \in \mathcal{U}$ presents an infeasible assignment of part i to printer m . We obtain set \mathcal{U} in preprocessing by checking for all parts whether a part exceeds the width, length, or height of the build space of m . In this check, the possibility of rotating a part 90 degrees around the z-axis is also taken into account. Consequently, (7) prohibits the assignment of items that have already been proven infeasible for placement on the specific machine. The completion times c_{bm} of batch b on machine m are defined by (8) and (9). According to the specifications laid out in Subsection 3.2, the completion time of a batch is determined by the setup time, the summed scan time to produce the total volume of the batch, and the time spent to cover the batch height with powder. With (9), we take into account the completion times of previous batches on the same machine. In (10), we use a modification of no-good cuts (Martello and Toth, 1990; Côté et al., 2021) to exclude infeasible batches of the sub-problem that is

a two-dimensional orthogonal packing problem with rotation (2D-OPR). By applying these constraints, we forbid the assignment of more than $|S|$ parts to a batch on machine m for subsets $S \in \mathcal{T}_m$ (Côté et al., 2021). Variable domains are given in (11)–(13).

We adopt the formulation of the unrelated machine environment used in Kucukkoc (2019) for our model. A new feature in the given model is the replacement of area constraints by Benders cuts (10). Because Kucukkoc (2019) focuses explicitly on scheduling for AM, the packing problem is relaxed by implementing area restrictions, allowing assignments only if the summed area of assigned parts is smaller than or equal to the machine's build area. In contrast to this approach, we use the generic formulation adopted from the recent paper of Côté et al. (2021) on the 2D-BPP. Because the evaluation of a given subset S being part of \mathcal{T}_m is NP-complete (Clautiaux, Carlier and Moukrim, 2007a), it is a very challenging task. In the following section, we illustrate our solution approach to the considered problem. In addition, we describe the detailed steps to determine whether a subset $S \in \mathcal{T}_m$ and therefore must be excluded from the solution space.

4. A branch-and-cut approach

4.1. Overall solution procedure

Figure 4 illustrates the proposed solution method. We consider (1)–(13) as the master problem, wherein no constraints of type (10) are initially imposed. To strengthen the formulated master problem, we conduct several preprocessing steps, apply additional constraints, and construct an initial solution for the problem instance. A detailed description of these improvements can be found in Subsection 4.2.

Subsequently, the algorithm solves the problem in a branch-and-cut manner by iteratively adding cuts to the model if necessary. For each solution candidate, we validate the current solution with regard to the feasibility of packed parts in a batch. To this end, we use a step-wise verification mechanism, which consists of lower bounding techniques, relaxation approaches, and the check for packing feasibility by solving the 2D-OPR. Subsection 4.3 provides detailed explanations of these strategies and their implementation. If an infeasible packing is found, we add a cut to the model and proceed with solving. If no violations can be identified for all used batches, the solution is feasible. The algorithm terminates if the optimal solution is found or if the time limit is reached.

4.2. Model improvements

4.2.1. Additional constraints

We extend the presented model with valid inequalities and fix variables to accelerate the solution process. We allow a total of B batches to be assigned to each available machine. Let \hat{B} denote the number of used batches on a specific machine. Consequently, the total number of possible choices for used batches is $\binom{B}{\hat{B}}$ (Che et al., 2021). To break this symmetry, we allow a batch b to be opened only if its predecessor $b - 1$ on the same machine is also used; we do so by adding inequalities

$$y_{b-1,m} \geq y_{bm} \quad \forall b \in \mathcal{B}, b > 0, m \in \mathcal{M}, \quad (14)$$

to the model of the master problem. We can further reduce symmetry by prohibiting the assignment of part i to batch b if $b > i$ – for example, part 1 is only allowed to be assigned to batch 1, while part 2 can be placed in batches 1 and 2, and so on. We integrate this specification for our problem of unrelated machines based on Côté et al. (2021) with

$$x_{ibm} = 0 \quad \forall b \in \mathcal{B}, i \in \mathcal{I}, b > i, m \in \mathcal{M}. \quad (15)$$

Constraints (16) limit the total area of all parts assigned to a batch b to be less than or equal to the available area A_m of machine m . These inequalities are typically used to model one-dimensional packing based on area (see, e.g., Kucukkoc, 2019; Rohaninejad et al., 2021) and to significantly reduce the number of checks in the sub-problem, since the verification mechanisms only need to be called for batches that satisfy the continuous lower bound.

$$\sum_{i \in \mathcal{I}} x_{ibm} \cdot \alpha_i \leq A_m \quad \forall b \in \mathcal{B}, m \in \mathcal{M}. \quad (16)$$

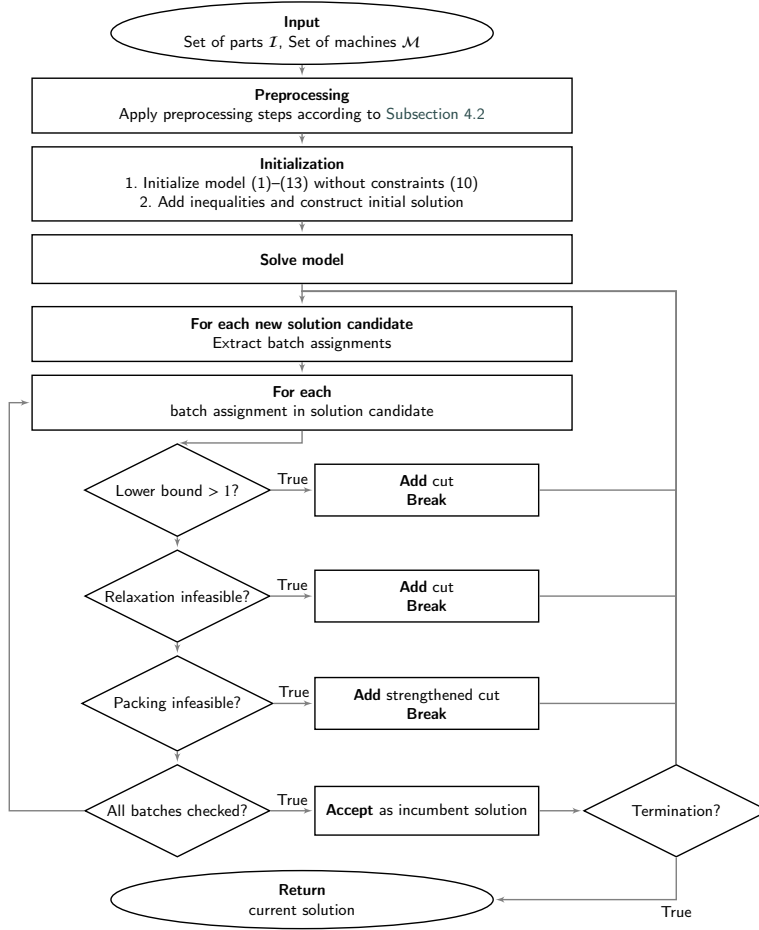


Figure 4: General Solution Strategy

Additionally, we define a set of incompatibilities. Let Q_m be a set of part tuples. A tuple $(i, j) \in Q_m$ establishes that part i and part j cannot be placed in the same batch on machine m , since they do not fit together in the build area of m . We determine all pairs in Q_m in the preprocessing step and add (17) to the model so as to allow only one of the parts in the same batch b on machine m . Note that incompatibilities must be defined for each machine individually, due to the machines being unrelated.

$$x_{ibm} + x_{jbm} \leq 1 \quad \forall b \in \mathcal{B}, i, j \in \mathcal{I}, m \in \mathcal{M}, i < j, (i, j) \in Q_m. \quad (17)$$

4.2.2. Reducing the number of available batches

In Subsection 3.2, we assume $I = B$ on each machine in order to ensure feasibility. This assumption leads to many unnecessary decision variables that need to be handled and thus to increased computational effort. We reduce the total batch number B with a heuristic procedure based on the first-fit decreasing height heuristic (Chung, Garey and Johnson, 1982; Berkey and Wang, 1987) without losing optimal solutions. Given a set of parts \mathcal{I} and a set of machines \mathcal{M} , the algorithm splits the studied problem into individual single machine problems, and for each machine $m \in \mathcal{M}$, we run the same steps, as follows. First, all parts that cannot be placed within the build area of m are discarded. Then, all remaining parts are rotated so that $\omega_i \geq \lambda_i$ and are sorted by decreasing part width. After that, we fill batches according to first-fit for the respective machine until all parts are assigned. We store the number of needed batches B_m for machine m . Finally, B is set to the maximum of all B_m – i.e., $B = \max_{m \in \mathcal{M}} \{B_m\}$.

4.2.3. Construction of initial solutions

To obtain a start solution, we first assign each part to a specific machine. Then, we construct batches in light of the given machine allocation of each part, using the principles of the first fit decreasing heuristic by Johnson (1973) with the extension by shelves (Baker and Schwarz, 1983). Algorithm 1 summarizes the procedure of finding a start solution to the studied problem. $\text{StartSolution}(\mathcal{B}, \mathcal{I}, \mathcal{M}, \mathcal{F})$ creates $|\mathcal{F}|$ different solutions, where \mathcal{F} represents a set of sorting strategies. In each for-loop, set \mathcal{I} is reordered in accordance with the respective sorting strategy, after which a start solution s_f is generated by applying the described steps of assigning parts to printers and forming batches on these printers. All potential start solutions are stored in set \mathcal{L} . Algorithm 1 returns the solution with the lowest makespan, computed with the function $\text{GetBestSolution}(\mathcal{L})$.

Algorithm 1: $\text{StartSolution}(\mathcal{B}, \mathcal{I}, \mathcal{M}, \mathcal{F})$

Input: Set of batches \mathcal{B} ; set of parts \mathcal{I} , set of machines \mathcal{M} , set of sorting strategies \mathcal{F}

Output: initial solution s

```

1  $\mathcal{L} \leftarrow \emptyset$ 
2 foreach  $f \in \mathcal{F}$  do
3   sort  $\mathcal{I}$  according to  $f$ 
4    $h_f \leftarrow \text{AssignPartsToMachines}(\mathcal{I}; \mathcal{M})$ 
5    $s_f \leftarrow \text{ConstructBatches}(\mathcal{B}; \mathcal{I}; \mathcal{M}; h_f)$ 
6    $\mathcal{L} \leftarrow \mathcal{L} \cup \{s_f\}$ 
7  $s \leftarrow \text{GetBestSolution}(\mathcal{L})$ 
8 return  $s$ 

```

The function $\text{AssignPartsToMachines}(\mathcal{I}; \mathcal{M})$ aims to balance the workload between the printers: given a set of parts \mathcal{I} and a set of machines \mathcal{M} , the algorithm first determines the possible machine assignments for each part using the set of infeasible part-machine assignments \mathcal{U} . Part i can only be assigned to machine m if $(i, m) \notin \mathcal{U}$. After all possible assignments are determined, each part is randomly allocated to one of the possible machines; the resulting assignment permutation h_f represents the starting point for a local search procedure that improves the assignment. A neighbor h'_f of a solution h_f is created by changing the machine assignment of one part $i \in \mathcal{I}$; hence, the size of the neighborhood of a solution is $(M - 1) \cdot I$. To evaluate the neighbors, we calculate the maximum workload by determining the processing times on each machine as if all assigned parts fit into one batch and then returning the maximum of all available machines. Thus, we do not consider the dimensions of the parts in this step. The algorithm returns the improved machine assignment permutation h_f .

After all parts have been allocated to one of the machines, batches are formed using the function $\text{ConstructBatches}(\mathcal{B}; \mathcal{I}; \mathcal{M}; h_f)$. This procedure begins by assigning the first part to the first batch on the respective machine based on h_f . The following parts are successively checked to determine if they fit into an already-existing batch. For checks with only two parts, we conduct a pairwise comparison in terms of rotation around z-axis; if a batch contains more than two parts, feasibility is evaluated using the shelf first-fit decreasing heuristic (Baker and Schwarz, 1983). If either of the two checks returns a feasible packing of the parts, the considered part is permanently assigned to the batch, and we resume the procedure with the next part. In case of no feasible packing in any existing batches, we open a new batch. This procedure continues until all parts have been placed. The resulting solution s_f is stored in set \mathcal{L} of all constructed solutions. Finally, the best start solution s is selected from among all solutions \mathcal{L} .

4.3. Evaluation of solution candidates

Whenever a solution candidate is found for model (1)–(13), its feasibility must be verified by checking each of its nonempty batches. Each nonempty batch of a solution contains a specific subset of parts $S \subseteq \mathcal{I}$. If any check determines that S is an infeasible batch for its associated machine m , we add no-good cuts (18) for all batches b of this specific machine m .

$$\sum_{i \in S} x_{ibm} \leq |S| - 1 \quad \forall b \in \mathcal{B}. \quad (18)$$

To guarantee the feasibility or infeasibility of a batch, a 2D-OPR must be solved. Since this is a computationally challenging problem (Côté et al., 2021), we want to avoid unnecessary calls to solve the actual 2D-OPR; instead, we try to prove the infeasibility of a batch as fast as possible. Consequently, we perform the verification of a given batch in multiple steps. First, we use a lower bound technique for the given batch, before we invoke two different relaxation approaches based on DFF and on the non-contiguous bin packing problem (NCBP) (Boschetti and Montaletti, 2010; Côté, Dell'Amico and Iori, 2014). If we cannot prove infeasibility of the given batch with these steps, we then solve the 2D-OPR with a CP model. The different procedures of the verification mechanism are explained in the following subsections.

4.3.1. Infeasibility by lower bounds

For each solution candidate, one or more batches are assigned to each machine. Each batch contains a specific subset of parts $S \subseteq \mathcal{I}$. The first step of our verification mechanism checks whether a batch is feasible by computing a lower bound. We use the bound presented in Dell'Amico et al. (2002), which is based on cutting the parts into squares to make rotations redundant. We denote the considered bound as LB_{DMV} . Given a set \mathcal{J} of square parts after the cutting procedure, subsets of parts S_1, S_2, S_{23}, S_3 , and S_4 are built depending on threshold q , s.t. $0 \leq q \leq \frac{\Lambda}{2}$, and the edge length of each part j given by $\lambda_j, j \in \mathcal{J}$. These sets are defined by

$$S_1 = \left\{ j \in \mathcal{J} : \lambda_j > \Omega - q \right\}, \quad (19)$$

$$S_2 = \left\{ j \in \mathcal{J} : \Omega - q \geq \lambda_j > \frac{\Lambda}{2} \right\}, \quad (20)$$

$$S_3 = \left\{ j \in \mathcal{J} : \frac{\Omega}{2} \geq \lambda_j > \frac{\Lambda}{2} \right\}, \quad (21)$$

$$S_{23} = \left\{ j \in S_2 \cup S_3 : \lambda_j > \Lambda - q \right\}, \quad (22)$$

$$S_4 = \left\{ j \in \mathcal{J} : \frac{\Lambda}{2} \geq \lambda_j \geq q \right\}. \quad (23)$$

It should be noted that we omit the machine indices of width Ω_m and length Λ_m for simplicity. In the model, the appropriate values for the machines Ω_m and Λ_m are used depending on the machine assignment of a batch. LB_{DMV} is calculated according to (24)–(26), where $\bar{S}_3 \subseteq S_3$ represents the set of parts in S_3 , which can be packed into the batches that pack the parts of S_2 (Dell'Amico et al., 2002).

$$\widetilde{LB} = |S_2| + \max \left\{ \left\lceil \frac{\sum_{j \in S_3 \setminus \bar{S}_3} \lambda_j}{\Omega} \right\rceil, \left\lceil \frac{|S_3 \setminus \bar{S}_3|}{\lfloor \frac{\Omega}{\lfloor \frac{\Lambda}{2} + 1 \rfloor} \rfloor} \right\rceil \right\}, \quad (24)$$

$$LB(q) = |S_1| + \widetilde{LB} + \max \left\{ 0, \left\lceil \frac{\sum_{j \in S_2 \cup S_3 \cup S_4} \lambda_j^2 - (\Omega \cdot \Lambda \cdot \widetilde{LB} - \sum_{j \in S_{23}} \lambda_j \cdot (\Lambda - \lambda_j))}{\Omega \cdot \Lambda} \right\rceil \right\}, \quad (25)$$

$$LB_{DMV} = \max_{0 \leq q \leq \frac{\Lambda}{2}} \{LB(q)\}. \quad (26)$$

Another bound, LB_{BM} , is presented in Boschetti and Mingozzi (2003). In contrast to LB_{DMV} , this bound explicitly takes into account the possible rotation of parts. Due to the time complexity of $O(n^3)$ for LB_{BM} in comparison to $O(\hat{n})$ for LB_{DMV} with $n = |S|, \hat{n} = |\mathcal{J}|$, we decided to only use LB_{DMV} (Boschetti and Mingozzi, 2003; Dell'Amico et al., 2002). If the resulting value for LB_{DMV} is greater than 1, we have found an infeasible assignment S and therefore add a no-good cut (18) to the master problem (1)–(13). Otherwise, the algorithm continues with the next feasibility check.

4.3.2. Infeasibility by orthogonal relaxation

In the second step, we try to prove the infeasibility of subset S using two different relaxation procedures. First, we consider a constraint satisfaction problem (CSP) with feasibility constraints built on DFF (see, e.g., Polyakovskiy and M'Hallah, 2018). A DFF represents a function $u : [0, 1] \rightarrow [0, 1]$, in which for any set \mathcal{K} of non-negative real numbers, there is a relation in accordance with inequality (27) (Fekete and Schepers, 2004).

$$\sum_{\kappa \in \mathcal{K}} \kappa \leq 1 \implies \sum_{\kappa \in \mathcal{K}} u(\kappa) \leq 1. \quad (27)$$

Given two DFFs u_1 and u_2 , we are able to transform the scaled width w'_i and length l'_i of part $i \in S$ into $(u_1(w'_i), u_2(l'_i))$, where $w'_i = w_i/W$ and $l'_i = l_i/L$. Let α_{ci} be a scaled area, where $\alpha_{ci} = u_1(w'_i) \cdot u_2(l'_i)$. A feasible packing is only possible if the sum of all scaled areas is less than or equal to one (Polyakovskiy and M'Hallah, 2018), i.e.,

$$\sum_{i \in S} \alpha_{ci} \leq 1. \quad (28)$$

Let $S^E = \{1, \dots, i, \dots, n, n+1, \dots, 2n\}$ be the set of parts in S augmented by the identical parts rotated by 90 degrees $(n+1, \dots, 2n)$. The decision variable d_i , $i \in S^E$, indicates whether part i is packed in the batch or not. In addition, C denotes the set of combined DFFs u_1 and u_2 . Using this notation, the CSP can be defined as:

$$\sum_{i \in S} (\alpha_{ci} \cdot d_i + \alpha_{c,n+i} \cdot d_{n+i}) \leq 1 \quad \forall c \in C, \quad (29)$$

$$d_i + d_{n+i} = 1 \quad \forall i \in S, \quad (30)$$

$$d_i \in \{0, 1\} \quad \forall i \in S^E. \quad (31)$$

We apply the functions $u^{(\epsilon)}$, $U^{(\epsilon)}$, and $\phi^{(\epsilon)}$ as presented in Fekete and Schepers (2004), where $\epsilon = \{p, q\}$, and we define the same combinations of these functions that the authors use for their bound L_{2d} . Additionally, we apply the combinations of DFFs from Fekete, Schepers and Van der Veen (2007) that are used for the check on orthogonal packings. If the model cannot be solved, we have found an infeasible subset S ; in this case, we add another cut (18) to the model and thus reject the solution candidate.

For the second relaxation procedure, we consider the adjusted version of the bin packing problem with contiguity constraints (ICBP). In the ICBP, each item i is cut into ω_i slices of length λ_i and width 1, and the bin size transforms into length Λ and width 1. The goal is to pack all slices into the minimum number of bins, under the condition that all slices of the same part i must be packed side-by-side with each other (Côté et al., 2014). This condition is omitted for the NCBP, which is also known as the bar relaxation (Belov, Kartak, Rohling and Scheithauer, 2013). To prohibit the stacking of slices of the same part $i \in I$, we require that at most one slice of each part is packed into the same bin.

The NCBP can be described as follows. A pattern t identifies a subset of parts whose summed length is less than or equal to the machine's length. Originally, the pattern is described by an array $(\sigma_{1t}, \dots, \sigma_{it}, \dots, \sigma_{nt})^T$, where σ_{it} is 1 if part i is in the pattern, and 0 otherwise (Côté et al., 2014). To account for the possible rotation of a part, we additionally allow σ_{it} to take the value of ω_i/λ_i if the part is rotated in the pattern. Let \mathcal{T} be the set of all currently available patterns that include at least one slice of an item, and let integer variable z_t denote how often a pattern t is used in the solution. Then, in accordance with Côté et al. (2014), the NCBP can be modeled as:

$$\sum_{t \in \mathcal{T}} z_t \rightarrow \min \quad (32)$$

s.t.:

$$\sum_{t \in \mathcal{T}} \sigma_{it} \cdot z_t \geq \omega_i \quad \forall i \in S, \quad (33)$$

$$z_t \in \mathbb{N}_{\geq 0} \quad \forall t \in \mathcal{T}. \quad (34)$$

In (32), we minimize the total number of used patterns. Constraints (33) ensure that the total number of appearances of each part i in all used patterns is greater than or equal to the part's width ω_i . (34) defines the domain of the decision variable z_t . Since the NCBP is an NP-hard problem, we follow Côté et al. (2014) and only consider the continuous relaxation of (32)–(34), for which we use the column generation approach presented by Gilmore and Gomory (1961) for the cutting stock problem. \mathcal{T} is initialized with n patterns, each of which incorporates a slice of one individual part i . To take into account the restriction that each pattern t can include only one slice of a part, as well as the possibility to rotate the parts, we adjust the sub-problem of the original column generation approach.

Let $S^E = \{1, \dots, i, \dots, n, n+1, \dots, 2n\}$ again be the set of parts in S augmented by their rotated versions. The binary variable v_i is 1 if a part i is in the solution of the sub-problem, and 0 otherwise. Given the dual values δ_i of (33), we define the sub-problem as:

$$1 - \left(\sum_{i=1}^n \delta_i \cdot v_i + \sum_{i=n+1}^{2n} \frac{\lambda_i}{\omega_i} \cdot \delta_i \cdot v_i \right) \rightarrow \min \quad (35)$$

s.t.:

$$\sum_{i \in S^E} v_i \lambda_i \leq L, \quad (36)$$

$$v_i + v_{i+n} \leq 1 \quad \forall i \in S, \quad (37)$$

$$v_i \in \{0, 1\} \quad \forall i \in S^E. \quad (38)$$

Similar to other column generation techniques, we seek to find a new pattern to add to the master problem, which we do by finding a combination of part slices that minimizes the objective function (35). To account for the rotation of part $i + n$, the dual value δ_i of part i is multiplied by the ratio λ_i/ω_i in the objective function. We ensure that the summed length of slices does not exceed the length of the machine with (36). Constraints (37) enforce that only one rotation for each part is used. Whenever the sub-problem is solved, we extract the found solution and create a new pattern to add to the master problem. As stated above, if a part i appears in the solution with its original orientation, we add 1 to the new pattern; in cases in which part i has been rotated, the value of this part in the considered pattern will be ω_i/λ_i .

We continue the search for new patterns until no better solution can be found. In this case, we compare the continuous lower bound of model (32)–(34) with the width of the machine to which the examined batch has been assigned. If the value of the lower bound is larger than the machine's width, we have found an infeasible subset S ; at this point, we add a cut of type (18) and continue the solution process of model (1)–(13).

4.3.3. Infeasibility by orthogonal packing

In cases in which the above-mentioned verification steps are not able to prove the infeasibility of a batch, we solve the 2D-OPR with CP as an exact method to ensure the infeasibility or feasibility of a batch. CP has already been proven to be suitable for two-dimensional orthogonal packing in several publications (see, e.g., Martello, Pisinger, Vigo, Boef and Korst (2007); Pisinger and Sigurd (2007); Clautiaux, Jouglet, Carlier and Moukrim (2008)). Recently, Polyakovskiy and M'Hallah (2021) use CP to solve the 2D-OPR sub-problem in a similar problem configuration.

To model the 2D-OPR as a CSP, we define variables x_i^S , x_i^E , y_i^S , and y_i^E to describe the start and end positions of a part i on the x-axis and on the y-axis, respectively. The variables w_i and l_i represent the width and length of a part i . We use the interval variables

$$\text{interval}_i^x \rightarrow x_i^S + w_i = x_i^E \quad \forall i \in S, \quad (39)$$

$$\text{interval}_i^y \rightarrow y_i^S + l_i = y_i^E \quad \forall i \in S, \quad (40)$$

to link the start and end points of part i on an axis with its respective dimension. Furthermore, the binary variable e_{ir} is 1 if part i is placed with rotation variant $r \in \mathcal{R}_i$, and 0 otherwise. Finally, ω_{ir} and λ_{ir} denote the width and the length,

respectively, of part i in rotation r . The CP model for the CSP can be formulated as follows:

$$\sum_{r \in \mathcal{R}_i} e_{ir} = 1 \quad \forall i \in \mathcal{S}, \quad (41)$$

$$\text{NoOverlap2D}(\{\text{interval}_i^x : i \in \mathcal{S}\}, \{\text{interval}_i^y : i \in \mathcal{S}\}), \quad (42)$$

$$e_{ir} = 1 \Rightarrow w_i = \omega_{ir} \wedge l_i = \lambda_{ir} \quad \forall i \in \mathcal{S}, r \in \mathcal{R}_i. \quad (43)$$

Constraints (41) ensure that exactly one orientation for each part is chosen. Constraint (42) is a global constraint and guarantees that all rectangles are non-overlapping. The rectangle associated with part i is defined by the combination of interval variables interval_i^x and interval_i^y . Constraints (43) determine the width and length of part i based on the selected rotation variant r . It should be noted that due to the consideration of rectangles and the possibility of rotating a part 90 degrees, the number of possible rotation variants is one if the part is represented as a square, and two otherwise.

In the following, we discuss the domains of the variables. Since there are at most two different rotation variants, the variables w_i and l_i can only take the width and length of the rotated or non-rotated part. Hence, the domains are defined according to

$$w_i \in \left\{ \min_{r \in \mathcal{R}_i} \{\omega_{ir}\}; \max_{r \in \mathcal{R}_i} \{\omega_{ir}\} \right\} \quad \forall i \in \mathcal{S}, \quad (44)$$

$$l_i \in \left\{ \min_{r \in \mathcal{R}_i} \{\lambda_{ir}\}; \max_{r \in \mathcal{R}_i} \{\lambda_{ir}\} \right\} \quad \forall i \in \mathcal{S}. \quad (45)$$

For the positioning variables x_i^S , x_i^E , y_i^S , and y_i^E , we reduce the solution space of the 2D-OPR by using the principle of minimal meet-in-the-middle patterns (MMIM) introduced by Côté and Iori (2018). To respect the rotation of parts, we adjust the procedures `MinimalMIMSet`($\mathcal{I}; \Omega$) and `NormalPatterns`($\mathcal{I}; \Omega$) presented by these authors. By adding another loop for rotations $r \in \mathcal{R}_i$ in line 4, `Algorithm 2` respects rotations in normal patterns. The resulting procedure is illustrated as `AdjustedNormalPatterns`($\mathcal{I}; \Omega$) in `Algorithm 2`. For `MinimalMIMSet`($\mathcal{I}; \Omega$), this is done by invoking `AdjustedNormalPatterns`($\mathcal{S} \setminus i; \Omega - \min_{r \in \mathcal{R}_i} \{\omega_{ir}\}$) taking into account the rotations on filling the arrays T^{left} , T^{right} , and defining the minimal set of placement points for part $i \in \mathcal{I}$. We display the pseudocode for `AdjustedMinimalMIMSet`($\mathcal{I}; \Omega$) in `Algorithm 3`. After the sets of placement points $\mathcal{P}_i^{\text{min},x}$ and $\mathcal{P}_i^{\text{min},y}$ are determined, the variable domains are defined as:

$$x_i^S = \left\{ p : p \in \mathcal{P}_i^{\text{min},x} \right\} \quad \forall i \in \mathcal{S}, \quad (46)$$

$$x_i^E = \left\{ p + \omega_{ir} : p \in \mathcal{P}_i^{\text{min},x}, r \in \mathcal{R}_i \mid p + \omega_{ir} \leq \Omega \right\} \quad \forall i \in \mathcal{S}, \quad (47)$$

$$y_i^S = \left\{ p : p \in \mathcal{P}_i^{\text{min},y} \right\} \quad \forall i \in \mathcal{S}, \quad (48)$$

$$y_i^E = \left\{ p + \lambda_{ir} : p \in \mathcal{P}_i^{\text{min},y}, r \in \mathcal{R}_i \mid p + \lambda_{ir} \leq \Lambda \right\} \quad \forall i \in \mathcal{S}. \quad (49)$$

If the CSP (41)–(43) ascertains the infeasibility of \mathcal{S} , we add another no-good cut. As noted by Côté et al. (2021), these cuts are usually weak for large sets \mathcal{S} ; thus, we prefer finding a minimal infeasible subset (MIS) $\mathcal{S}' \subseteq \mathcal{S}$ that cannot be packed onto machine m . Using \mathcal{S}' instead of \mathcal{S} in no-good cuts (18) would lead to a strengthened cut.

However, finding an MIS is a challenging task. Therefore, we apply the heuristic approach from Côté et al. (2021) of finding a reduced infeasible subset (RIS). First, the parts in \mathcal{S} are sorted by ascending area. Then, we iteratively remove the smallest part from the subset and invoke model (41)–(43) with the reduced set \mathcal{S}' and a time limit. The procedure continues as long as infeasibility can be proved for \mathcal{S}' . If infeasibility cannot be proven within the time limit or if the considered subset is feasible, we reinsert the last removed part i into \mathcal{S}' and use \mathcal{S}' to generate a new cut.

Algorithm 2: AdjustedNormalPatterns($\mathcal{I}; \Omega$) in accordance with Côté and Iori (2018)

Input: set of parts \mathcal{I} , machine width Ω
Output: set of placement points \mathcal{N}_0 according to normal pattern principle

```

1  $T \leftarrow [0 \text{ to } \Omega]$ : all entries initialized as 0
2  $T[0] \leftarrow 1$ 
3 foreach  $i \in \mathcal{I}$  do
4   foreach  $r \in \mathcal{R}_i$  do
5     foreach  $p = \Omega - \omega_{ir}$  to 0 do
6       if  $T[p] = 1$  then
7          $T[p + \omega_{ir}] \leftarrow 1$ 
8  $\mathcal{N}_0 \leftarrow \emptyset$ 
9 foreach  $p = \Omega$  to 0 do
10  if  $T[p] = 1$  then
11   $\mathcal{N}_0 \leftarrow \mathcal{N}_0 \cup \{p\}$ 
12 return  $\mathcal{N}_0$ 

```

5. Computational experiments

In this section, we analyze the performance of the proposed B&C approach. We consider two variants of the algorithm: the first is the original approach B&C^{Org}, described in the previous section; the second is a two-step procedure called B&C^{TS}. In the first step, we try to improve the initial solution by invoking B&C^{Org} with a more restricted version of constraint (16), such that the summed part areas in a batch are at most 90% of the respective machine area. In the second step, we use the improved initial solution as a start solution for the original approach with 100% occupation of machine areas. With this adjusted B&C, we attempt to avoid getting stuck in checking very dense packings, which are not likely to be part of an optimal solution in the unrestricted version. We compare both variants to the MIP model presented by Che et al. (2021), since this is the only other exact solution approach addressing rectangular shapes and unrelated machines; we denote this model as MIP^{Che}. During preliminary testing, we observed some irregularities in the MIP model, as some packing problems with a known feasible solution were declared infeasible. After thorough investigation, we solved these issues by correcting the Big-M values used in the model. The MIP^{Che} model and a comprehensive explanation of the changes can be found in the supplementary material to this study.

The B&C approaches have been implemented with GUROBI and GOOGLE OR-TOOLS in PYTHON. We use the former to model the master problem and the orthogonal relaxation procedures, while we use the latter to implement the CP model of the 2D-OPR. The MIP^{Che} is also modeled using PYTHON and GUROBI.

We evaluate the performance of the approaches using two different data sets. First, we use the data given in Che et al. (2021), which is available online (Che et al., 2021); then, we analyze the given data set, point out some drawbacks, and propose a new comprehensive test data set. This data set is used to analyze the solution approaches in more detail.

The study is conducted on an AMD EPYC 7513 with 3.0 GHz clock speed and 64 GB RAM. For the computational tests, the maximum number of threads is set to eight, and an overall time limit of 3,600 seconds is defined for the adjusted MIP^{Che} model and both B&C variants. To comply with the overall time limit in the B&C approaches, we dynamically set the time limit of the CP model in the feasibility check of a batch to the residual runtime (3,600 sec minus the elapsed time). GUROBI's relative MIP optimality gap is set to $7 \cdot 10^{-6}$. The evaluation of a potential cut strengthening in B&C is restricted to two seconds. With regard to the B&C^{TS}, the maximum time spent in the restricted version of the master problem is set to 10% of the overall computation time (i.e., 360 sec). All test runs are repeated three times with different seed values.

5.1. Comparative tests on existing test data

5.1.1. Instance data

As stated in Section 2, Che et al. (2021) study a problem configuration for packing and scheduling in AM that is similar to the problem in this paper. In addition to rotation around the z-axis, the authors also allow a subset of orientations around the x- and y-axes. Table 1 presents the given data for an example part. Each part is defined with up to three

Algorithm 3: AdjustedMinimalMIMSet($\mathcal{I}; \Omega$) in accordance with Côté and Iori (2018)

Input: set of parts \mathcal{I} , machine width Ω
Output: minimal set \mathcal{P} of MIM placement points

```

1  $T^{\text{left}}, T^{\text{right}} \leftarrow [0 \text{ to } W]$ : all entries initialized as 0
2 foreach  $i \in \mathcal{I}$  do
3    $\mathcal{V}_i \leftarrow \text{AdjustedNormalPatterns}(S \setminus i; \Omega - \min_{r \in \mathcal{R}_i} \{\omega_{ir}\})$ 
4   foreach  $p \in \mathcal{V}_i$  do
5      $T^{\text{left}}[p] = 1$ 
6     foreach  $r \in \mathcal{R}_i$  do
7       if  $\omega_{ir} < \Omega$  then
8          $T^{\text{right}}[\Omega - \omega_{ir} - p] \leftarrow T^{\text{right}}[\Omega - \omega_{ir} - p] + 1$ 
9   foreach  $p = 1$  to  $\Omega$  do
10     $T^{\text{left}}[p] \leftarrow T^{\text{left}}[p] + T^{\text{left}}[p - 1]$ 
11     $T^{\text{right}}[\Omega - p] \leftarrow T^{\text{right}}[\Omega - p] + T^{\text{right}}[\Omega - (p - 1)]$ 
12   $t^{\text{min}} \leftarrow 1$ 
13   $\text{min} \leftarrow T^{\text{left}}[0] + T^{\text{right}}[1]$ 
14  foreach  $p = 2$  to  $\Omega$  do
15    if  $T^{\text{left}}[p - 1] + T^{\text{right}}[p] < \text{min}$  then
16       $\text{min} \leftarrow T^{\text{left}}[p - 1] + T^{\text{right}}[p]$ 
17       $t^{\text{min}} \leftarrow p$ 
18   $\mathcal{P} \leftarrow \emptyset$ 
19  foreach  $i \in \mathcal{I}$  do
20     $\mathcal{P}_i \leftarrow \emptyset$ 
21    foreach  $p \in \mathcal{V}_i$  do
22      if  $p < t^{\text{min}}$  then
23         $\mathcal{P}_i \leftarrow \mathcal{P}_i \cup \{p\}$ 
24        foreach  $r \in \mathcal{R}_i$  do
25          if  $\Omega - \omega_{ir} - p \geq t^{\text{min}}$  then
26             $\mathcal{P}_i \leftarrow \mathcal{P}_i \cup \{\Omega - \omega_{ir} - p\}$ 
27     $\mathcal{P} \leftarrow \mathcal{P} \cup \mathcal{P}_i$ 
28 return  $\mathcal{M}$ 
    
```

	Width	Length	Height	Support volume
Orientation				
1	6	2	28	10
2	2	28	6	2
3	6	28	2	0

Table 1

Description of model part data in Che et al. (2021)

Type	W_m	L_m	H_m	T_m^{recoat}	T_m^{scan}	T_m^{setup}
1	25.0	25.0	32.5	0.7	0.030864	2
2	40.0	80.0	50.0	0.25	0.030864	1
3	40.0	40.0	40.0	0.14	0.030864	1
4	40.0	60.0	45.0	0.16	0.030864	1

Table 2

Description of machine data from Che et al. (2021)

different orientations, resulting in different parameter values for its width, length, and height, as well as for the needed support structure. The original part data is collected from the website Thingiverse (www.thingiverse.com), which provides user-produced design data. The authors use four different machine types based on the parameters of Kucukkoc (2019) and Li et al. (2017); the types differ in the dimensions of the building platform, setup times, and recoating times T_m^R (see Table 2). Che et al. (2021) define seven classes of instances, ranging from 20 parts and two machines to 500 parts and seven machines. We focus on the instance classes with 20 and 50 parts (Class 1 and 2), each containing 20 instances, since Che et al. (2021) have solved them with their integrated MIP model. The remaining instance classes have only been solved with a simulated annealing approach.

To adapt the instances of Che et al. (2021) to our problem setting, we fix the orientation for each part in advance by considering the calculation of the completion times of a batch in constraints (8) and (9). Despite minor variations due to different support volumes, the choice of orientation does not affect the volume-dependent aspect of the processing time. However, taller parts directly influence the height of a batch and thus directly influence the processing time; hence, to speed up the printing process, parts should be designed so that they can be printed with the largest area lying on the build plate. We apply the Minimum-Height-Up (MHU) rule to decide which orientation to take: for example, the application of MHU would result in orientation 3 for the part in Table 1. The respective support volume is added to the total volume v_i of each part i .

5.1.2. Results

The general results of all solution approaches for each instance are displayed in Table 3. First, we find that all instances of class 1 are optimally solved by all approaches. However, in comparisons of the average computation times T^{avg} , we observe clear advantages of B&C^{Org} and B&C^{TS}: on average, both B&C variants need less than 50% of the computation time needed for MIP^{Che} to prove optimality. Looking at the results for class 2, we see that the MIP^{Che} can only prove optimality in at least one run of four instances; in contrast, B&C^{Org} and B&C^{TS} provide proven optimal solutions in at least one run for five and six instances, respectively. In general, both B&C variants yield considerably better lower and upper bounds in the best run than the model MIP^{Che}. However, for B&C^{Org}, we observe a large deviation between the best and the average optimality gaps for some instances (e.g., 2, 9, and especially 15). In contrast, B&C^{TS} provides significantly smaller gap values on average and smaller deviations between the best and average values.

In what follows, we examine the results in more detail to determine the reasons for these performance differences between the B&C variants. To this end, Table 4 provides information about the times spent in the different feasibility checks of the algorithms. We use the following notations: #E represents the number of explored batch assignments; T_{LB} , T_{OR} , T_{BR} , and T_{OP} represent the total computation times of the lower bound (LB), orthogonal relaxation (OR), bar relaxation (BR), and orthogonal packing (OP) verification methods; $t_{\text{OP}}^{\text{max}}$ denotes the maximum time spent for a single orthogonal packing problem averaged by all seed runs; and #HP reports the number of hard packing instances. We define a hard packing instance as an orthogonal packing problem that takes at least 300 sec to be solved in the CP model. All numbers represent average values over three seed runs. It should be noted that we can only terminate the algorithm after checking an integer solution; therefore, total times of slightly more than 3,600 sec may also be reported.

First, we observe that in both approaches, only a small computational effort is used for the relaxed orthogonal packing checks LB, OR, and BR. In most instances, the main share of the computation time is spent in the exact 2D-OPR check: column $t_{\text{OP}}^{\text{max}}$ shows that in several problem instances, the available computation time is nearly entirely consumed by a single check of the 2D-OPR. However, in some instances (e.g., 2, 5, 6, 8, 13) the variant B&C^{TS} spends significantly less time in the exact 2D-OPR check, and $t_{\text{OP}}^{\text{max}}$ is greatly reduced. Additionally, we observe that the number of hard packing instances is slightly reduced in the variant B&C^{TS}. Thus, it can be deduced that the original variant B&C^{Org} gets stuck more often in the exact check of batches very early in the solution process; as a result, the lower and upper bounds cannot improve as much as they do in the variant B&C^{TS}. We also can see that hard packing instances are not necessarily part of an optimal solution. For example, instances 8 and 13 can be solved to optimality with B&C^{TS} in fast computation times, while B&C^{Org} spends much time in the exact 2D-OPR check. Providing a better initial solution can thus be beneficial, since it helps to prune the search tree.

We further investigate the hard packing instances to identify possible reasons for why the CP solver cannot decide whether a 2D-OPR instance is feasible or infeasible in a reasonable time. Following Clautiaux et al. (2007a), we calculate measure ϵ for each packing problem with the set of parts S on a machine m that has a runtime of at least 300 sec, where $\sum_{i \in S} a_i = (1 - \epsilon) \cdot A_m$, meaning that ϵ measures the free area when considering a specific batch. Figure 5 shows the aggregated results as scatter plots, with measures ϵ and $|S|$ segmented by the different machine types. All hard-to-solve packing problems except one have ϵ values below 3%, implying a high packing density between 97 – 100% in the considered batches. These results are consistent with the findings of Clautiaux et al. (2007a), but difficult instances are slightly skewed toward lower ϵ . The authors show in their computational experiments that a high area utilization is associated with increased computational difficulty and therefore impacts whether a packing problem can be solved in a reasonable time. Examining the different machine types, we observe that most hard packing problems occur on machine type 1 with the smallest build platform, while fewer hard packing instances are seen with increasing production areas of machine types. For the machine type 4, the largest in terms of the build area, no hard packing

No.	B&C ^{Org}							B&C ^{TS}						
	#E	T_{LB}	T_{OR}	T_{BR}	T_{OP}	t_{OP}^{max}	#HP	#E	T_{LB}	T_{OR}	T_{BR}	T_{OP}	t_{OP}^{max}	#HP
1	18.33	0.19	1.59	11.91	8.81	1.81	0.00	4.00	0.02	0.24	1.10	1.57	1.47	0.00
2	33.67	0.20	0.90	12.98	2976.67	2916.53	1.00	23.67	0.12	0.59	5.26	1168.33	1142.50	0.33
3	19.33	0.13	0.57	9.62	3580.42	3548.95	1.00	9.33	0.08	0.26	2.92	3572.70	3530.21	1.00
4	28.00	0.08	0.80	7.10	3583.47	3562.15	1.00	17.00	0.09	0.53	9.19	3538.37	3359.60	1.33
5	17.33	0.21	0.65	20.94	2170.35	2163.00	0.67	4.00	0.03	0.15	4.75	2.64	2.50	0.00
6	18.00	0.22	0.87	13.81	1223.32	1209.46	0.33	4.00	0.03	0.13	1.95	1.46	0.84	0.00
7	15.67	0.21	0.74	16.24	6.06	1.14	0.00	4.67	0.05	0.19	4.65	1.26	0.89	0.00
8	26.00	0.12	0.49	8.79	3577.22	1716.33	2.33	22.33	0.07	0.65	6.19	114.75	98.76	0.00
9	21.67	0.09	0.73	9.57	3585.00	3576.43	1.00	11.67	0.04	0.39	6.32	3547.91	3341.29	1.33
10	32.67	0.19	0.76	8.41	3582.20	3169.94	1.33	14.00	0.09	0.38	5.26	3551.57	3435.25	1.00
11	29.00	0.13	1.12	9.98	3572.14	3068.59	1.33	10.00	0.03	0.37	1.85	3574.18	3464.07	1.00
12	28.67	0.16	0.96	10.26	3568.76	2460.56	2.33	9.67	0.03	0.31	3.73	3556.50	3379.45	1.33
13	22.67	0.10	0.59	5.92	3579.56	3535.79	1.00	15.67	0.09	0.48	1.90	34.99	34.03	0.00
14	32.00	0.14	1.04	9.37	3584.15	3521.32	1.00	16.33	0.11	0.48	5.58	3390.62	3181.37	1.33
15	12.00	0.08	0.28	3.55	3594.60	3158.34	1.33	10.67	0.08	0.31	3.54	3564.32	3535.48	1.00
16	20.00	0.30	1.23	24.71	6.85	1.10	0.00	4.00	0.04	0.16	3.67	0.93	0.56	0.00
17	20.00	0.19	0.58	4.06	3592.15	3281.80	1.33	10.33	0.06	0.26	1.22	1077.48	1075.05	0.33
18	19.00	0.14	1.08	10.65	3582.76	3018.78	1.33	12.67	0.11	0.66	3.61	3475.80	3179.99	1.33
19	12.67	0.15	0.38	9.61	3589.09	3554.51	1.00	9.00	0.12	0.27	9.94	3229.04	3086.27	1.00
20	30.33	0.21	1.48	21.41	3130.76	1971.02	2.33	12.00	0.09	0.60	5.45	3541.27	3379.32	1.33

#E: Number of batches checked. T_{LB} : Total computation time spent on lower bounds, T_{OR} : Total computation time spent on orthogonal relaxation, T_{BR} : Total computation time spent on bar relaxation, T_{OP} : Total computation time spent on orthogonal packing, t_{OP}^{max} : Maximum computation time spent on orthogonal packing, #HP: Number of hard packing instances with $T_{OP} > 300$.

Table 4
Detailed information on computation times for Class 2 instances

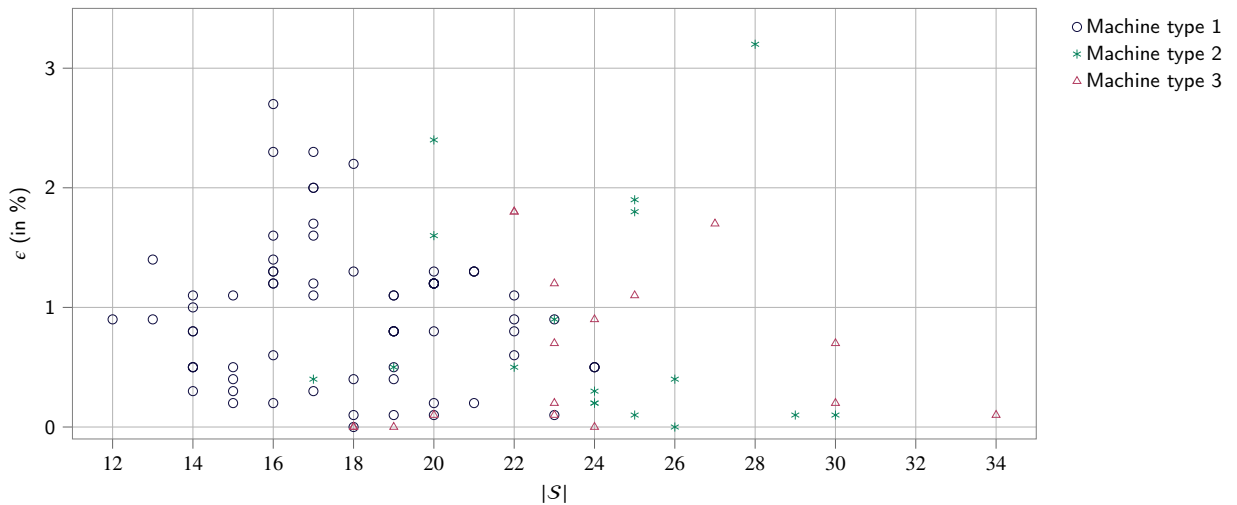


Figure 5: Scatter plot representing ϵ values and item numbers of hard packing instances ($T_{OP} > 300$ sec.) for the B&C variants

instance is detected in the experiments. Additionally, the number of parts in the hard packing problems indicates that the parts are small compared to the machine area. To validate this assumption, we give a more detailed overview of the instances introduced by Che et al. (2021) in the following section. We also analyze other instance sets used for scheduling in additive manufacturing in order to give a broader perspective.

5.2. Generation of new benchmark instances

5.2.1. Discussion on instance data used for scheduling in additive manufacturing

We examine the data from various studies on AM scheduling to gain insights on the part dimensions they use. Table 5 shows selected problem data for planning in AM that is either accessible online via provided links or explicitly explained in the studies. The first column presents the source of the problem data, and column #Parts describes the total number of parts evaluated. The next five columns present the evaluation of part areas: this begins with the

Reference	data set	#D	#Parts	Part areas α_i (in cm^2)					Part area shares (in %)		
				$\bar{\alpha}_i$	$P_{25\%}$	$P_{50\%}$	$P_{75\%}$	$\max \alpha_i$	$\frac{\bar{\alpha}_i}{\min\{A_m\}}$	$S_{50\%}$	$S_{25\%}$
Rohaninejad et al. (2021)	-	1	1985	500.64	399.24	500.08	601.04	966.44	59.13	31.34	2.27
Che et al. (2021)	<i>ht1</i>	2	400	73.10	25.00	38.22	88.00	289.80	10.14	100.00	86.25
Che et al. (2021)	<i>ht2</i>	2	1000	65.46	25.00	38.00	68.89	289.80	7.81	100.00	91.70
Kucukkoc (2019)	<i>SM</i>	1	126	213.45	91.35	248.92	269.75	709.06	28.79	89.68	42.86
Kucukkoc (2019)	<i>IM</i>	1	638	227.61	89.68	174.43	270.44	980.08	20.59	88.09	75.86
Kucukkoc (2019)	<i>UM</i>	1	638	227.61	89.68	174.43	270.44	980.08	28.16	85.42	60.03
Chergui et al. (2018)	-	2	20	67.51	15.08	35.65	51.88	361.00	10.80	90.00	90.00

#D: Number of dimensions in packing, #Parts: Number of evaluated part specifications, $\bar{\alpha}_i$: Avg. part area, $P_{25\%}$: 25% percentile of part area within the test data, $P_{50\%}$: 50% percentile of part area within the test data, $P_{75\%}$: 75% percentile of part area within the test data, $\max \alpha_i$: maximum part area within the test data, $\frac{\bar{\alpha}_i}{\min\{A_m\}}$: Avg. area consumption of one part based on the minimum machine area, $S_{50\%}$: Share of parts that are smaller than 50% of the minimum machine area in the test data, $S_{25\%}$: Share of parts that are smaller than 25% of the minimum machine area in the test data.

Table 5

Comparison of part data of available test data in literature on scheduling in additive manufacturing

average part area $\bar{\alpha}_i$, followed by percentiles and the maximum part area of the considered data displayed in columns $P_{25\%}$, $P_{50\%}$, $P_{75\%}$, and $\max_{i \in I} \alpha_i$. The remaining columns of the table report shares relative to the minimum machine area of each problem instance: the first column in this section presents the average share of area taken up by a part, while the last two columns indicate the share of parts that are smaller than 50% and 25% of the minimum build area, respectively.

Table 5 reports the smallest part areas for the data of Chergui et al. (2018) and Che et al. (2021). This applies for both the absolute part areas and the relative areas with regard to the minimum machine area. Comparing the interquartile ranges of those data sets to the ones from Kucukkoc (2019), we can further deduce less diversity in part sizes in the data of Chergui et al. (2018) and Che et al. (2021). Evaluating the relative part areas to the minimum machine area, we see that the majority of parts occupy less than 25% of the minimum machine area.

Based on these findings, we see two drawbacks of the used test set. First, a test set should comprise a diverse set of instances in order to study, e.g., the influences of different part sizes on the solution process and the solution quality. A more diversified benchmark data set that takes into account varying part dimensions may also more precisely represent real-world requirements in AM shops. Second, test instances with a majority of small parts might make solving for the proposed B&C more difficult, because many techniques for preprocessing, lower bounds determination, and domain reduction leverage parts that are larger than 50% of the bin dimensions. Thus, these techniques have no effect on the instances of Che et al. (2021); the effectiveness of the proposed B&C variants cannot be tested properly with the test data, since the approaches get stuck early in the search. As can be seen in Table 5, all of the remaining available data assumes one-dimensional packing. Consequently, a new benchmark data set is needed for planning in AM, one that incorporates different part sizes in accordance with the well-known benchmark data for cutting and packing problems (see, e.g., Berkey and Wang, 1987; Martello and Vigo, 1998). We propose such a new benchmark data set in the next section.

5.2.2. Description of new test instances

We first define the machine system and the part sizes for the new test data. The structure of the available machines is explained in Table 10 in the appendix. As regards the dimensions of the machines' build spaces, we follow the product data sheets of machine manufacturers (see, e.g., SLM Solutions AG, 2023) and the machine specifications from related work (Kucukkoc, 2019; Che et al., 2021). We randomly draw machine parameters from the intervals shown in the table to generate the process speed parameters; these intervals are also based on manufacturers' product data sheets. We then use the formulas proposed by Aloui and Hadj-Hamou (2021) to calculate scanning and recoating times.

As regards part sizes, we follow the approach of Martello and Vigo (1998), who define different part types and create classes in which certain types of parts occur more frequently. This allows us to generate a diverse set of parts. Furthermore, we can examine the solution behavior of the algorithms based on different part sizes. Table 6 gives a detailed explanation of the four part types and the classes of the test data. According to the definition, classes 1 and 2 contain rather small parts, while classes 3 and 4 comprise bigger parts, and the parts in classes 2 and 3 tend to be more elongated compared to those in classes 1 and 4. Finally, we define the test instances in Table 7, resulting in 36

Part type 1	uniformly random integers: ω_i in $[1, \frac{1}{5}\Omega]$, λ_i in $[1, \frac{1}{5}\Lambda]$, h_i in $[1, \frac{1}{2}H]$
Part type 2	uniformly random integers: ω_i in $[1, \frac{1}{5}\Omega]$, λ_i in $[\frac{1}{5}\Lambda, \frac{3}{5}\Lambda]$, h_i in $[1, \frac{1}{2}H]$
Part type 3	uniformly random integers: ω_i in $[\frac{1}{5}\Omega, \frac{2}{5}\Omega]$, λ_i in $[\frac{1}{5}\Lambda, \frac{4}{5}\Lambda]$, h_i in $[1, \frac{1}{2}H]$
Part type 4	uniformly random integers: ω_i in $[\frac{3}{5}\Omega, \frac{5}{5}\Omega]$, λ_i in $[\frac{3}{5}\Lambda, \frac{5}{5}\Lambda]$, h_i in $[1, \frac{1}{2}H]$
Class 1	part type 1 with probability 70%, type 2, 3, 4 with probability 10% each. $\Omega = \Lambda = H = 50$
Class 2	part type 2 with probability 70%, type 1, 3, 4 with probability 10% each. $\Omega = \Lambda = H = 50$
Class 3	part type 3 with probability 70%, type 1, 2, 4 with probability 10% each. $\Omega = \Lambda = H = 50$
Class 4	part type 4 with probability 70%, type 1, 2, 3 with probability 10% each. $\Omega = \Lambda = H = 500$

Table 6

Definition of part types and classes

Parameter and levels for test data generation							
Parameters	Levels					Total	
		I					
	M	10	20	40	60	80	
Combinations of parts and machines	2	X	X	X	X	X	9
	3		X	X			
	5				X	X	
Number of part classes	1, 2, 3, 4					4	
	Total number of configurations					36	
	Number of instances/ configuration					5	
	Number of problem instances					180	
	Number of runs/ instance					3	
	Total number of experiments					540	

Table 7

Parameters and their levels for test data and parameter tuning

configurations and a total of 180 problem instances. For each instance, we ensure that the build space of machine type 1 is included for at least one machine; the remaining machine build spaces are drawn randomly from the available types in Table 10. In this way, we ensure that each part fits in at least one machine.¹

5.3. Results for new benchmark instances

Figure 6 presents an overview of the test results, reporting the optimality gaps at the termination of each method; the results are segmented by classes, number of parts I , and number of machines M . More detailed results for the different approaches are given in Table 8.² Overall, we deduce from Figure 6 that both B&C variants generate superior results to the MIP model for almost all configurations. This superiority is especially pronounced for larger instance sizes. As a result, the decomposition is particularly useful for instances with larger problem sizes. For the MIP^{Che} model, we can see a sharp increase in the optimality gaps as the number of parts increases across all classes; in contrast, the optimality gaps of both B&C variants grow only moderately with the instance size. For classes 1 and 2, both B&C variants generate better results than MIP^{Che}, but the variant B&C^{TS} provides significantly smaller MIP gaps than B&C^{Org}. In these classes, MIP^{Che} produces MIP gaps up to 72% for the largest instances, whereas B&C^{Org} and B&C^{TS} result in average gaps below 20% and below 10%, respectively. For classes 3 and 4, we see that the MIP gaps of both B&C variants are larger and more uniform than those in classes 1 and 2, while the MIP gaps of MIP^{Che} are mostly smaller than those in classes 1 and 2; thus, the overall benefits of the B&C variants decrease. However, it is only for the largest problem size of class 4 that no performance advantages of the B&C variants over MIP^{Che} can be seen.

¹All test instances are available online via:

<https://data.mendeley.com/datasets/k4vrvbf5kb/draft?a=07c17363-17e5-424f-9aa9-d59328005ae0>

²A comprehensive summary of all test results can be found in the supplementary materials of this manuscript. The individual output files are available online via: <https://data.mendeley.com/datasets/k4vrvbf5kb/draft?a=07c17363-17e5-424f-9aa9-d59328005ae0>

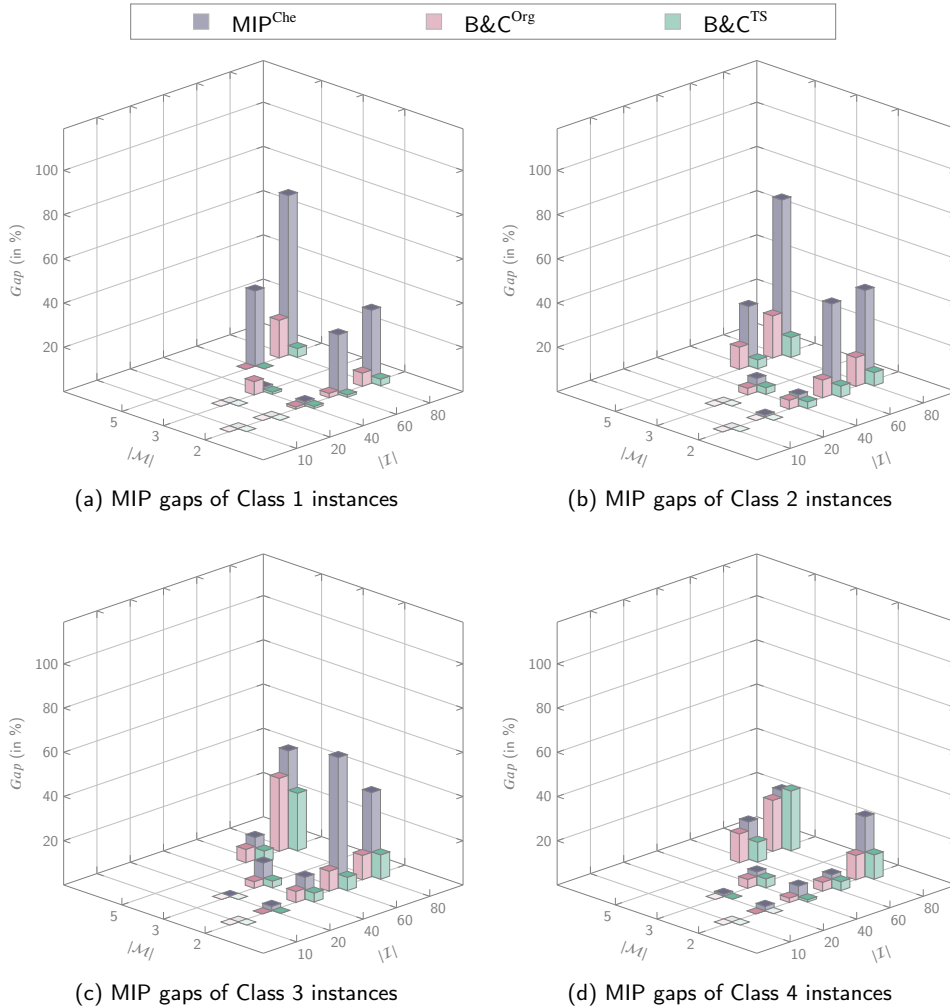


Figure 6: 3D bar plots illustrating the resulting optimality gaps by classes, item numbers, and machine numbers

The reason for these differences is the varying relevance of both problems in additive manufacturing – i.e., packing and scheduling. Recall that classes 1 and 2 include small parts; thus, more parts are packed into a single batch, and fewer batches are needed to produce all parts. Here, on the one hand, the packing problem is more relevant and harder to solve, while on the other hand, the scheduling problem (i.e., which batch is produced on which machine at which time) is less important, since fewer batches results in fewer possibilities to combine batches. For classes 3 and 4, fewer parts fit into a batch, which means more batches are required. Here, the scheduling decision is crucial, while the packing feasibility check is easier and less relevant. Since the master problem manages the scheduling decisions, the results of the B&C variants and MIP^{Che} are more similar in classes 3 and 4. We also hypothesize that the obtained lower bounds in classes 3 and 4 are weaker than those in classes 1 and 2 due to the more prominent scheduling problem. In the comparison of the B&C variants, the better optimality gaps of $B\&C^{TS}$ in classes 1 and 2 are primarily the result of better upper bounds of the final solutions in $B\&C^{TS}$. These improved upper bounds result from better initial solutions by invoking the more restricted problem first, and better initial solution prevent the algorithm in $B\&C^{TS}$ from checking lower-quality solutions with dense packings. In this way, compared to $B\&C^{Org}$, $B\&C^{TS}$ is able to check more solutions with better upper bounds.

These findings are supported by the detailed analysis of the added cuts and the time needed to check feasibility (see Table 9). For classes 1 and 2, a large share of the total runtime is spent in the feasibility check, whereas for classes

3 and 4, this share is much smaller, even though far more batches are checked. We can also observe that fewer batches are explored for instances with 80 parts compared to instances with 60 parts for classes 3 and 4. Solving the continuous relaxation at each node of the branch-and-bound tree becomes computationally more demanding with increasing instance size; as a result, fewer nodes and fewer integer solutions can be explored, which in turn leads to a deterioration of the solution quality for larger instances.

With regard to the added cuts, the simple lower bounds are ineffective for instances with smaller parts but are useful if the parts are larger. In contrast, the orthogonal relaxation procedure can prove infeasibility for a large share of batches across all classes. Despite the preceding orthogonal relaxation using DFFs, the bar relaxation also generates a substantial number of cuts and prevents the algorithm from unnecessary calls of the 2D-OPR. Evaluating the different classes, we see that the bar relaxation is more advantageous with larger parts. The improved initial solution in B&C^{TS} significantly impacts the number of explored batches #E and, consequently, the check time. Except for the instances with 80 parts in classes 3 and 4, B&C^{TS} demonstrates a significantly lower time spent on feasibility checks than B&C^{Org}.

6. Conclusion

This study is motivated by the planning processes in additive manufacturing, where several parts can be simultaneously processed together in the same batch on a 3D printer. We investigate the integrated problem of two-dimensional orthogonal packing with rotation and scheduling on unrelated parallel machines. In order to solve this problem exactly, we propose a new branch-and-cut approach, in which we use and extend several adaptations of state-of-the-art procedures and techniques from the packing literature. In extensive computational tests on several data sets, we assess two variants of the proposed branch-and-cut and demonstrate their superior algorithmic performance compared to an integrated mixed-integer programming model taken from the literature. In addition, we analyze the structure of existing test data for scheduling in additive manufacturing and propose a new benchmark test set. Using this new benchmark set, we show that the size of parts greatly impacts whether the scheduling problem or the packing problem is more prominent. In a comprehensive evaluation of the test results, we find that using dual feasible functions can effectively prove infeasibility of packing sub-problems. This is especially the case in comparison with lower bound techniques, which only add significant value in the solution process for instances with larger parts. In summary, the considered stepwise procedure prevented the algorithm from invoking other feasibility checks, which are more costly in terms of computational effort.

The proposed algorithms struggle to determine feasibility or infeasibility for packing sub-problems with many parts that are small relative to the build area. To improve early infeasibility detection, reduction techniques that exist for the packing problem variant with fixed orientation should be extended to the case with rotation. For practitioners, several problem extensions must be explored in order to improve real-world applicability. For example, considering minimum distances between processed parts enables ensuring a certain level of printing quality. Considering irregularly-shaped parts enables increases in build space utilization. Similarly, extending the sub-problem to a 3D packing problem enables higher build space utilization for additive manufacturing technologies that allow the stacking of parts. Furthermore, the considered solution procedures may be applied to other related problems – for example, the two-dimensional bin packing problem with rotation or the two-dimensional orthogonal packing problem with rotation. Further studies should show the extent to which incorporating these methods can improve the existing benchmark results.

Cl.	I	M	#runs	MIP ^{Che}					B&C ^{Org}					B&C ^{TS}						
				U^{sum}	L^{sum}	G^{avg}	T^{avg}	#o	U_0^{sum}	U^{sum}	L^{sum}	G^{avg}	T^{avg}	#o	U_0^{sum}	U^{sum}	L^{sum}	G^{avg}	T^{avg}	#o
1	10	2	15	400.44	400.44	0.00	0.37	15	413.00	400.44	400.44	0.00	0.40	15	400.44	400.44	400.44	0.00	0.52	15
	20	2	15	333.18	333.18	0.00	3.81	15	352.02	333.18	333.18	0.00	1.97	15	333.18	333.18	333.18	0.00	1.70	15
		3	15	371.66	371.66	0.00	7.74	15	497.16	371.66	371.66	0.00	4.51	15	371.80	371.66	371.66	0.00	5.42	15
	40	2	15	819.55	806.27	1.78	2922.79	3	923.65	817.75	813.41	0.94	1950.17	9	820.37	817.93	812.54	0.97	1910.90	8
		3	15	939.25	930.03	1.57	2219.14	6	1216.49	959.48	928.14	6.25	1492.87	9	937.88	936.16	933.50	0.67	1231.02	11
	60	2	15	2748.81	1650.81	27.33	3431.97	3	1958.92	1734.05	1708.13	1.69	2669.16	5	1731.65	1725.53	1712.68	0.84	2884.98	3
		5	15	3914.39	444.26	33.97	2946.50	6	828.93	471.26	471.21	0.01	2185.40	6	471.84	471.26	471.22	0.01	2196.12	6
	80	2	15	3455.56	2136.54	33.44	3600.33	0	2564.01	2341.20	2188.16	5.81	3602.18	0	2266.03	2261.30	2193.57	2.63	3600.78	0
		5	15	8869.13	635.44	72.37	3600.30	0	1139.63	777.34	682.88	10.88	3601.17	0	724.41	718.63	690.79	4.08	3601.16	0
	2	10	2	15	262.80	262.80	0.00	0.38	15	289.28	262.80	262.80	0.00	0.51	15	263.24	262.80	262.80	0.00	0.60
20		2	15	650.18	646.63	0.61	1327.87	10	735.88	648.91	648.91	0.00	34.55	15	655.87	648.91	648.91	0.00	33.54	15
		3	15	486.49	486.49	0.00	55.07	15	624.70	486.49	486.49	0.00	10.35	15	488.27	486.49	486.49	0.00	13.75	15
40		2	15	1560.58	1490.98	4.90	3349.67	2	1709.00	1551.33	1509.13	3.48	2884.32	3	1631.65	1539.82	1508.01	2.58	2885.24	3
		3	15	932.66	872.40	6.44	3600.74	0	1306.83	913.99	888.14	2.88	3600.87	0	913.42	909.70	889.02	2.47	3401.18	1
60		2	15	3619.80	1762.20	40.96	3601.29	0	2185.17	1990.27	1828.42	8.08	3601.32	0	1926.58	1925.29	1828.52	4.88	3600.87	0
		5	15	1835.50	877.22	27.21	3512.13	1	1523.55	998.01	903.16	9.55	2194.78	6	944.08	939.41	909.54	3.68	2195.39	6
80		2	15	5440.44	2658.27	41.93	3600.24	0	3368.21	3184.02	2780.14	13.33	3600.77	0	2953.38	2951.43	2793.33	5.67	3600.86	0
		5	15	11716.41	1003.81	69.98	3600.60	0	1750.67	1335.01	1065.16	18.79	3601.10	0	1175.29	1172.12	1065.98	8.81	3600.65	0
3		10	2	15	1090.17	1090.17	0.00	4.33	15	1125.32	1090.17	1090.17	0.00	1.05	15	1090.17	1090.17	1090.17	0.00	1.33
	20	2	15	1543.75	1506.88	2.42	2951.92	3	1791.62	1542.79	1538.31	0.19	873.18	12	1543.60	1542.79	1538.12	0.20	886.52	12
		3	15	1324.31	1323.69	0.06	920.51	14	1613.60	1324.31	1324.31	0.00	39.91	15	1328.88	1324.31	1324.31	0.00	56.76	15
	40	2	15	2593.24	2346.40	9.69	3600.43	0	2927.91	2584.92	2458.66	4.83	3600.63	0	2576.07	2566.41	2464.83	3.88	3600.42	0
		3	15	1817.38	1626.78	10.14	3600.49	0	2385.57	1786.19	1737.70	2.87	3600.55	0	1791.05	1783.76	1740.60	2.49	3600.39	0
	60	2	15	11477.57	3140.18	59.11	3600.43	0	3849.91	3641.43	3323.75	8.47	3593.49	1	3622.28	3560.31	3326.08	6.39	3600.51	0
		5	15	1944.24	1779.20	9.50	3172.28	3	3050.93	1942.50	1838.62	6.08	2891.80	3	1976.12	1928.44	1843.69	5.04	2912.93	3
	80	2	15	12802.34	6539.05	37.60	3601.13	0	7887.26	7643.68	6807.73	11.08	3600.95	0	7811.17	7652.87	6805.83	11.17	3600.62	0
		5	15	6506.24	2003.49	43.60	3600.54	0	3664.65	3183.77	2129.40	32.82	3600.85	0	3094.88	2862.02	2132.01	25.97	3600.78	0
	4	10	2	15	900.07	900.07	0.00	1.40	15	998.15	900.07	900.07	0.00	0.87	15	900.07	900.07	900.07	0.00	0.98
20		2	15	1474.73	1453.28	1.48	2880.62	3	1643.90	1474.32	1473.88	0.03	1102.13	13	1477.04	1474.32	1474.32	0.00	1081.49	15
		3	15	1225.08	1215.71	0.61	1939.18	8	1550.94	1225.08	1225.08	0.00	571.73	15	1225.91	1225.08	1225.08	0.00	667.41	15
40		2	15	2926.95	2794.80	5.87	2802.07	6	3371.45	2908.20	2874.51	1.56	2227.70	6	2908.12	2902.08	2875.95	1.22	2274.84	6
		3	15	1896.24	1789.37	5.96	3600.86	0	2583.84	1886.98	1813.90	3.96	3600.46	0	1887.00	1877.35	1815.24	3.46	3600.34	0
60		2	15	5008.15	4693.89	6.40	3602.67	0	5411.16	4941.90	4746.74	4.02	3601.14	0	4997.54	4927.10	4750.20	3.48	3600.90	0
		5	15	2158.35	1769.79	17.12	3600.69	0	3074.79	2116.96	1849.74	13.39	3600.95	0	2097.69	2024.03	1850.70	8.95	3600.83	0
80		2	15	7574.95	5269.63	27.08	3600.44	0	6296.40	6016.62	5377.15	10.73	3600.93	0	6153.56	5984.27	5379.73	10.87	3600.91	0
		5	15	2506.50	1835.31	26.21	3600.38	0	2905.83	2524.22	1922.26	22.62	3600.96	0	3141.59	2729.09	1922.24	26.89	3601.21	0
Tot.				540	115127.07	60847.15	17.37	2557.26	173	79520.32	68311.33	62701.55	5.68	2187.38	223	68632.15	67226.56	62771.34	4.10	2184.83

U^{sum} : Sum of upper bounds, L^{sum} : Sum of lower bounds, G^{avg} : Avg. MIP Gap (in %), T^{avg} : Avg. runtime, #o: Number of optimal solved runs, U_0^{sum} : Sum of objective values of initial solutions.

Table 8
Detailed results of new benchmark tests categorized by classes, part numbers, and machine numbers

Cl.	I	M	#runs	B&C ^{Org}									B&C ^{TS}								
				#E	Cuts _{LB}	Cuts _{OR}	Cuts _{BR}	Cuts _{OP}	T_c^{avg}	t_{OP}^{max}	#HP	#E	Cuts _{LB}	Cuts _{OR}	Cuts _{BR}	Cuts _{OP}	T_c^{avg}	t_{OP}^{max}	#HP		
1	10	2	15	11.80	0.00	0.00	0.00	0.00	0.30	0.03	0.00	4.93	0.00	0.00	0.00	0.00	0.08	0.03	0.00		
	20	2	15	17.73	0.00	0.00	0.00	0.00	1.33	0.05	0.00	4.00	0.00	0.00	0.00	0.00	0.15	0.04	0.00		
	3	15	29.67	0.00	0.80	0.00	2.40	2.26	0.09	0.00	8.93	0.00	0.60	0.00	1.40	0.71	0.04	0.00			
	40	2	15	52.53	0.00	3.73	2.40	19.73	1194.65	768.02	0.80	26.33	0.00	1.67	1.53	9.47	1092.11	949.95	0.53		
	3	15	111.80	3.73	17.40	5.07	18.53	1181.44	978.01	0.60	79.60	3.60	21.20	13.27	20.33	677.63	538.09	0.47			
	60	2	15	454.13	0.20	178.60	20.53	152.47	1757.12	1277.19	0.87	256.60	0.13	109.00	16.53	90.20	1477.26	1083.87	0.60		
	5	15	155.60	0.00	40.53	2.13	60.93	211.98	104.58	0.07	69.20	0.00	21.93	0.80	35.67	201.71	122.39	0.07			
	80	2	15	225.60	0.00	93.20	4.53	54.60	2923.19	2263.82	1.53	95.27	0.00	33.00	4.27	27.47	2471.12	2142.25	1.20		
	5	15	222.33	0.00	95.60	10.93	85.13	2725.66	2371.09	1.27	210.20	0.00	84.60	10.73	71.33	1342.45	1015.90	0.73			
	2	10	2	15	10.87	0.00	0.00	0.00	0.00	0.32	0.03	0.00	4.40	0.00	0.00	0.00	0.09	0.03	0.00		
20		2	15	43.40	0.00	0.53	0.53	17.73	27.51	10.97	0.00	22.07	0.00	0.47	0.13	11.53	25.92	16.31	0.00		
3		15	66.73	0.00	11.33	1.33	24.53	2.75	0.11	0.00	27.93	0.00	5.00	0.00	20.07	1.52	0.09	0.00			
40		2	15	641.53	0.00	747.20	4.47	176.07	1781.60	1539.80	0.60	401.33	0.00	486.87	1.47	103.47	2033.40	1528.13	1.07		
3		15	696.67	0.00	476.07	24.27	376.67	1922.57	1436.20	0.87	421.93	0.00	291.93	14.87	216.33	1499.54	1219.49	0.60			
60		2	15	293.00	1.00	99.60	12.00	124.93	3324.43	1956.03	2.27	106.73	0.67	27.13	5.33	43.73	2973.48	2248.27	1.53		
5		15	420.73	0.00	318.27	25.20	263.47	1131.48	807.89	0.67	311.80	0.00	196.87	13.40	195.60	339.39	158.22	0.33			
80		2	15	766.87	0.00	878.93	19.53	270.00	2544.51	1757.97	1.60	515.00	0.00	636.93	17.93	172.27	2017.49	1359.91	1.40		
5		15	324.27	3.20	309.67	24.33	260.80	1675.42	1423.86	0.93	262.27	4.93	224.07	12.80	219.07	1099.27	877.92	0.60			
3		10	2	15	37.87	0.00	20.67	0.00	14.20	0.48	0.03	0.00	19.13	0.00	12.53	0.00	8.73	0.23	0.03	0.00	
	20	2	15	531.73	7.20	359.53	27.47	132.93	8.30	0.06	0.00	391.73	7.20	343.60	24.53	114.93	6.28	0.07	0.00		
	3	15	182.67	2.93	93.67	1.93	32.20	2.09	0.05	0.00	57.60	2.00	46.00	1.60	15.20	0.70	0.03	0.00			
	40	2	15	2557.80	27.20	2627.73	82.27	494.67	91.18	0.93	0.00	1683.13	21.13	1990.07	52.00	285.53	48.71	0.84	0.00		
	3	15	1469.40	33.47	1288.20	45.53	363.60	47.76	1.24	0.00	743.13	20.40	749.40	14.20	149.40	18.96	0.53	0.00			
	60	2	15	1021.40	14.13	765.93	41.60	189.93	224.08	174.99	0.07	957.33	11.20	750.80	42.93	156.27	48.55	13.81	0.00		
	5	15	911.40	0.00	1425.13	35.73	147.27	10.57	0.09	0.00	634.20	0.00	1044.53	11.20	71.80	6.57	0.08	0.00			
	80	2	15	820.80	0.00	1144.93	15.87	140.87	72.33	14.35	0.00	695.27	0.00	946.40	10.00	102.80	234.03	162.26	0.13		
	5	15	569.13	1.20	1508.73	14.20	51.40	8.33	0.15	0.00	488.40	0.40	1257.93	10.07	42.27	7.17	0.14	0.00			
	4	10	2	15	24.07	0.07	3.93	0.00	1.40	0.37	0.03	0.00	10.20	0.00	2.20	0.00	0.80	0.12	0.02	0.00	
20		2	15	352.87	0.00	319.40	5.07	77.73	7.45	0.21	0.00	289.33	0.00	306.20	2.53	52.27	4.49	0.05	0.00		
3		15	212.60	1.73	96.80	11.87	11.80	2.02	0.03	0.00	137.53	1.33	73.47	12.40	7.60	1.06	0.03	0.00			
40		2	15	1598.67	53.53	1056.27	13.80	113.20	36.56	0.33	0.00	983.40	36.67	708.47	6.13	44.33	15.61	0.26	0.00		
3		15	1467.60	5.87	2135.27	22.87	312.40	51.87	0.82	0.00	690.33	2.60	1225.60	8.87	122.93	18.36	0.39	0.00			
60		2	15	2221.27	0.00	2985.60	17.47	285.73	83.09	0.77	0.00	1478.27	0.00	2129.07	10.73	148.33	42.25	0.57	0.00		
5		15	1171.20	12.53	2062.67	15.13	143.73	21.91	0.37	0.00	863.80	8.53	1322.00	9.60	71.80	11.32	0.27	0.00			
80		2	15	1075.87	23.33	1450.60	19.40	151.20	176.76	91.03	0.13	842.33	17.27	895.53	12.13	112.87	248.23	208.65	0.13		
5		15	515.87	9.40	699.60	2.87	54.00	9.15	1.13	0.00	439.07	5.60	596.80	4.40	42.47	6.77	0.19	0.00			

#E: Number of batches checked, $Cuts_{LB}$, $Cuts_{OR}$, $Cuts_{BR}$, $Cuts_{OP}$: Avg. number of cuts, T_c^{avg} : Avg. runtime, T_c^{avg} : Avg. check time, #T/O: Number of runs with timeout within orthogonal packing.

Table 9

Cut analysis of B&C approaches categorized by classes and part numbers

Machine Build Spaces			
	Ω	Λ	H
Machine type 1	40	40	25
Machine type 2	25	25	20
Machine type 3	28	28	24
Machine type 4	28	28	32
Machine type 5	40	40	20
Machine type 6	28	50	36
Determination of processing times			
Scan speed σ	uniformly random integers in $[8, 11] \cdot 1,000 \frac{mm}{s}$		
Layer production speed ϕ	uniformly random integers in $[3, 7] \frac{s}{\text{layer}}$		
Laser diameter δ	uniformly random integers in $[8, 11] \cdot \frac{1}{100} mm$		
Layer thickness θ	uniformly random integers in $[4, 10] \cdot \frac{1}{100} mm$		
Setup time T_m^S	uniformly random in $[1, 2] h$		
Scanning time T_m^L	$T_m^L = \frac{1}{\sigma \cdot \delta \cdot \theta} \frac{h}{cm^3}$		
Recoating time T_m^R	$T_m^R = \frac{\phi}{\theta} \frac{h}{cm}$		

Table 10
Definition of machine parameters

A. Details on Machine Parameters

The following Table 10 presents the considered specifications and formulas, which are used to define the machine types and the individual parameters of each machine.

CRedit authorship contribution statement

Benedikt Zipfel: Conceptualization, Methodology, Software, Validation, Formal analysis, Investigation, Visualization, Writing - Original Draft, Writing - Review & Editing. **Felix Tamke:** Conceptualization, Methodology, Validation, Writing - Review & Editing. **Leopold Kuttner:** Conceptualization, Writing - Review & Editing.

References

- Alicastro, M., Ferone, D., Festa, P., Fugaro, S., Pastore, T., 2021. A reinforcement learning iterated local search for makespan minimization in additive manufacturing machine scheduling problems. *Computers & Operations Research* 131, 105272. doi:10.1016/j.cor.2021.105272.
- Aloui, A., Hadj-Hamou, K., 2021. A heuristic approach for a scheduling problem in additive manufacturing under technological constraints. *Computers & Industrial Engineering* 154, 107115. doi:https://doi.org/10.1016/j.cie.2021.107115.
- Arroyo, J.E.C., Leung, J.Y.T., 2017a. An effective iterated greedy algorithm for scheduling unrelated parallel batch machines with non-identical capacities and unequal ready times. *Computers & Industrial Engineering* 105, 84–100. doi:10.1016/j.cie.2016.12.038.
- Arroyo, J.E.C., Leung, J.Y.T., 2017b. Scheduling unrelated parallel batch processing machines with non-identical job sizes and unequal ready times. *Computers & Operations Research* 78, 117–128. doi:10.1016/j.cor.2016.08.015.
- Attaran, M., 2017. The rise of 3-D printing: The advantages of additive manufacturing over traditional manufacturing. *Business Horizons* 60, 677–688. doi:https://doi.org/10.1016/j.bushor.2017.05.011.
- Bain, E.D., 2019. Polymer powder bed fusion additive manufacturing: Recent developments in materials, processes, and applications, in: *Polymer-Based Additive Manufacturing: Recent Developments*. chapter 2, pp. 7–36. doi:10.1021/bk-2019-1315.ch002.
- Baker, B.S., Schwarz, J.S., 1983. Shelf algorithms for two-dimensional packing problems. *SIAM Journal on Computing* 12, 508–525. doi:10.1137/0212033.
- Baldacci, R., Boschetti, M.A., Ganovelli, M., Maniezzo, V., 2014. Algorithms for nesting with defects. *Discrete Applied Mathematics* 163, 17–33. doi:https://doi.org/10.1016/j.dam.2012.03.026. *mathheuristics* 2010.
- Belov, G., Kartak, V.M., Rohling, H., Scheithauer, G., 2013. Conservative scales in packing problems. *OR spectrum* 35, 505–542. doi:10.1007/s00291-011-0277-9.
- Berkey, J.O., Wang, P.Y., 1987. Two-dimensional finite bin-packing algorithms. *Journal of the Operational Research Society* 38, 423–429. doi:10.1057/jors.1987.70.
- Boschetti, M.A., Mingozzi, A., 2003. The two-dimensional finite bin packing problem. part II: New lower and upper bounds. *Quarterly Journal of the Belgian, French and Italian Operations Research Societies* 1, 135–147. doi:10.1007/s10288-002-0006-y.
- Boschetti, M.A., Montaletti, L., 2010. An exact algorithm for the two-dimensional strip-packing problem. *Operations Research* 58, 1774–1791. doi:10.1287/opre.1100.0833.
- Che, Y., Hu, K., Zhang, Z., Lim, A., 2021. Machine scheduling with orientation selection and two-dimensional packing for additive manufacturing. *Computers & Operations Research* 130, 105245. doi:10.1016/j.cor.2021.105245.

- Chergui, A., Hadj-Hamou, K., Vignat, F., 2018. Production scheduling and nesting in additive manufacturing. *Computers & Industrial Engineering* 126, 292–301. doi:10.1016/j.cie.2018.09.048.
- Chung, F.R.K., Garey, M.R., Johnson, D.S., 1982. On packing two-dimensional bins. *SIAM Journal on Algebraic Discrete Methods* 3, 66–76. doi:10.1137/0603007.
- Clautiaux, F., Carlier, J., Moukrim, A., 2007a. A new exact method for the two-dimensional orthogonal packing problem. *European Journal of Operational Research* 183, 1196–1211. doi:https://doi.org/10.1016/j.ejor.2005.12.048.
- Clautiaux, F., Jouglet, A., Carlier, J., Moukrim, A., 2008. A new constraint programming approach for the orthogonal packing problem. *Computers & Operations Research* 35, 944–959. doi:10.1016/j.cor.2006.05.012.
- Clautiaux, F., Jouglet, A., El Hayek, J., 2007b. A new lower bound for the non-oriented two-dimensional bin-packing problem. *Operations Research Letters* 35, 365–373. doi:10.1016/j.orl.2006.07.001.
- Côté, J.F., Dell'Amico, M., Iori, M., 2014. Combinatorial benders' cuts for the strip packing problem. *Operations Research* 62, 643–661. doi:10.1287/opre.2013.1248.
- Côté, J.F., Haouari, M., Iori, M., 2021. Combinatorial benders decomposition for the two-dimensional bin packing problem. *INFORMS Journal on Computing* 33, 963–978. doi:10.1287/ijoc.2020.1014.
- Côté, J.F., Iori, M., 2018. The meet-in-the-middle principle for cutting and packing problems. *INFORMS Journal on Computing* 30, 646–661. doi:10.1287/ijoc.2018.0806.
- Dell'Amico, M., Martello, S., Vigo, D., 2002. A lower bound for the non-oriented two-dimensional bin packing problem. *Discrete Applied Mathematics* 118, 13–24. doi:10.1016/S0166-218X(01)00253-0.
- Fekete, S.P., Schepers, J., 2004. A general framework for bounds for higher-dimensional orthogonal packing problems. *Mathematical Methods of Operations Research* 60, 311–329. doi:10.1007/s001860400376.
- Fekete, S.P., Schepers, J., Van der Veen, J.C., 2007. An exact algorithm for higher-dimensional orthogonal packing. *Operations Research* 55, 569–587. doi:10.1287/opre.1060.0369.
- Gardan, J., 2017. Additive manufacturing technologies: state of the art and trends, in: *Additive Manufacturing Handbook: Product Development for the Defense Industry*. 1 ed., chapter 10, pp. 149–168. doi:10.1201/9781315119106.
- Gibson, I., Rosen, D., Stucker, B., Khorsani, M., 2021. *Additive manufacturing technologies*. 3 ed., Springer Cham. doi:10.1007/978-3-030-56127-7.
- Gilmore, P.C., Gomory, R.E., 1961. A linear programming approach to the cutting-stock problem. *Operations Research* 9, 849–859. doi:10.1287/opre.9.6.849.
- Guo, N., Leu, M.C., 2013. Additive manufacturing: technology, applications and research needs. *Frontiers of Mechanical Engineering* 8, 215–243. doi:10.1007/s11465-013-0248-8.
- Hu, K., Che, Y., Zhang, Z., 2022. Scheduling unrelated additive manufacturing machines with practical constraints. *Computers & Operations Research* 144, 105847.
- Iori, M., de Lima, V.L., Martello, S., Miyazawa, F.K., Monaci, M., 2021. Exact solution techniques for two-dimensional cutting and packing. *European Journal of Operational Research* 289, 399–415. doi:10.1016/j.ejor.2020.06.050.
- Johnson, D.S., 1973. Near-optimal bin packing algorithms. Ph.D. thesis. Massachusetts Institute of Technology.
- Kang, H.S., Noh, S.D., Son, J.Y., Kim, H., Park, J.H., Lee, J.Y., 2018. The FaaS system using additive manufacturing for personalized production. *Rapid Prototyping Journal* 24, 1486–1499. doi:10.1108/RPJ-11-2016-0195.
- Kapadia, M.S., Starly, B., Thomas, A., Uzsoy, R., Warsing, D., 2019. Impact of scheduling policies on the performance of an additive manufacturing production system. *Procedia Manufacturing* 39, 447–456. doi:10.1016/j.promfg.2020.01.388.
- Kucukkoc, I., 2019. MILP models to minimise makespan in additive manufacturing machine scheduling problems. *Computers & Operations Research* 105, 58–67. doi:10.1016/j.cor.2019.01.006.
- Li, Q., Kucukkoc, I., Zhang, D.Z., 2017. Production planning in additive manufacturing and 3D printing. *Computers & Operations Research* 83, 157–172. doi:10.1016/j.cor.2017.01.013.
- Li, X., Huang, Y., Tan, Q., Chen, H., 2013. Scheduling unrelated parallel batch processing machines with non-identical job sizes. *Computers & Operations Research* 40, 2983–2990. doi:10.1016/j.cor.2013.06.016.
- Manco, P., Macchiaroli, R., Maresca, P., Fera, M., 2019. The Additive Manufacturing Operations Management Maturity: a Closed or an Open Issue? *Procedia Manufacturing* 41, 98–105. doi:10.1016/j.promfg.2019.07.034.
- Martello, S., Pisinger, D., Vigo, D., Boef, E.D., Korst, J., 2007. Algorithm 864: General and robot-packable variants of the three-dimensional bin packing problem. *ACM Transactions on Mathematical Software (TOMS)* 33, 7–es.
- Martello, S., Toth, P., 1990. *Knapsack problems: algorithms and computer implementations*. John Wiley & Sons, Inc.
- Martello, S., Vigo, D., 1998. Exact solution of the two-dimensional finite bin packing problem. *Management Science* 44, 388–399. doi:10.1287/mnsc.44.3.388.
- Oh, Y., Witherell, P., Lu, Y., Sprock, T., 2020. Nesting and Scheduling Problems for Additive Manufacturing: A Taxonomy and Review. *Additive Manufacturing* 36, 101492. doi:10.1016/j.addma.2020.101492.
- Pisinger, D., Sigurd, M., 2005. The two-dimensional bin packing problem with variable bin sizes and costs. *Discrete Optimization* 2, 154–167. doi:https://doi.org/10.1016/j.disopt.2005.01.002.
- Pisinger, D., Sigurd, M., 2007. Using decomposition techniques and constraint programming for solving the two-dimensional bin-packing problem. *INFORMS Journal on Computing* 19, 36–51. doi:10.1287/ijoc.1060.0181.
- Polyakovskiy, S., M'Hallah, R., 2018. A hybrid feasibility constraints-guided search to the two-dimensional bin packing problem with due dates. *European Journal of Operational Research* 266, 819–839. doi:https://doi.org/10.1016/j.ejor.2017.10.046.
- Polyakovskiy, S., M'Hallah, R., 2021. Just-in-time two-dimensional bin packing. *Omega* 102, 102311. doi:10.1016/j.omega.2020.102311.
- Rohaninejad, M., Hanzálek, Z., Tavakkoli-Moghaddam, R., 2021. Scheduling of parallel 3d-printing machines with incompatible job families: A matheuristic algorithm, in: *IFIP International Conference on Advances in Production Management Systems*, Springer. pp. 51–61.

- SLM Solutions AG, 2023. Product Information SLM 500. https://www.slm-solutions.com/fileadmin/Content/Machines/SLM_R_500_Web.pdf. Accessed: 2023-02-01.
- Tavakkoli-Moghaddam, R., Shirazian, S., Vahedi-Nouri, B., 2020. A Bi-objective Scheduling Model for Additive Manufacturing with Multiple Materials and Sequence-Dependent Setup Time, in: Lalic, B., Majstorovic, V., Marjanovic, U., von Cieminski, G., Romero, D. (Eds.), *Advances in Production Management Systems. Towards Smart and Digital Manufacturing*, Springer International Publishing, Cham. pp. 451–459. doi:10.1007/978-3-030-57997-5_52.
- Thompson, M.K., Moroni, G., Vaneker, T., Fadel, G., Campbell, R.I., Gibson, I., Bernard, A., Schulz, J., Graf, P., Ahuja, B., Martina, F., 2016. Design for additive manufacturing: Trends, opportunities, considerations, and constraints. *CIRP Annals* 65, 737–760. doi:10.1016/j.cirp.2016.05.004.
- Uzsoy, R., 1994. Scheduling a single batch processing machine with non-identical job sizes. *International Journal of Production Research* 32, 1615–1635. doi:10.1080/00207549408957026.
- Zhang, J., Yao, X., Li, Y., 2020. Improved evolutionary algorithm for parallel batch processing machine scheduling in additive manufacturing. *International Journal of Production Research* 58, 2263–2282. doi:10.1080/00207543.2019.1617447.
- Zipfel, B., Neufeld, J.S., Buscher, U., 2021. Customer order scheduling in an additive manufacturing environment, in: Dolgui, A., Bernard, A., Lemoine, D., von Cieminski, G., Romero, D. (Eds.), *Advances in Production Management Systems. Artificial Intelligence for Sustainable and Resilient Production Systems*, Springer International Publishing, Cham. pp. 101–109. doi:10.1007/978-3-030-85910-7_11.